1521-0111/92/5/533–545$25.00
MOLECULAR PHARMACOLOGY

https://doi.org/10.1124/mol.117.109249
Mol Pharmacol 92:533–545, November 2017

Prostaglandin E_2 Inhibits Histamine-Evoked Ca^{2+} Release in Human Aortic Smooth Muscle Cells through Hyperactive cAMP Signaling Junctions and Protein Kinase A[S]

Emily J. A. Taylor, Evangelia Pantazaka, Kathryn L. Shelley, and Colin W. Taylor

Department of Pharmacology, University of Cambridge, Cambridge, United Kingdom

Received May 2, 2017; accepted August 23, 2017

ABSTRACT

In human aortic smooth muscle cells, prostaglandin E_2 (PGE_2) stimulates adenylyl cyclase (AC) and attenuates the increase in intracellular free Ca^{2+} concentration evoked by activation of histamine H_1 receptors. The mechanisms are not resolved. We show that cAMP mediates inhibition of histamine-evoked Ca^{2+} signals by PGE_2. Exchange proteins activated by cAMP were not required, but the effects were attenuated by inhibition of cAMP-dependent protein kinase (PKA). PGE_2 had no effect on the Ca^{2+} signals evoked by protease-activated receptors, heterologously expressed muscarinic M3 receptors, or by direct activation of inositol 1,4,5-trisphosphate (IP_3) receptors by photolysis of caged IP_3. The rate of Ca^{2+} removal from the cytosol was unaffected by PGE_2, but PGE_2 attenuated histamine-evoked IP_3 accumulation. Substantial inhibition of AC had no effect on the concentration-dependent inhibition of Ca^{2+} signals by PGE_2 or butaprost (to activate EP_2 receptors selectively), but it modestly attenuated responses to EP_4 receptors, activation of which generated less cAMP than EP_2 receptors. We conclude that inhibition of histamine-evoked Ca^{2+} signals by PGE_2 occurs through "hyperactive signaling junctions," wherein cAMP is locally delivered to PKA at supersaturating concentrations to cause uncoupling of H_1 receptors from phospholipase C. This sequence allows digital signaling from PGE_2 receptors, through cAMP and PKA, to histamine-evoked Ca^{2+} signals.

Introduction

Ca^{2+} and cAMP are ubiquitous intracellular messengers that regulate most cellular behaviors. The versatility of these messengers depends on both the spatiotemporal organization of the changes in their concentration within cells (Cooper and Tabbasum, 2014) and on interactions between them [see references in Tovey et al. (2008)]. These interactions are important in many smooth muscles, where increases in intracellular free Ca^{2+} concentration ($[Ca^{2+}]_i$) stimulate contraction, but receptors that stimulate formation of cAMP usually cause relaxation. The clinical importance is clear from the widespread use of β-agonists to provide symptomatic relief from asthma (Morgan et al., 2014). In vascular smooth muscle (VSM), too, cAMP attenuates the contractile responses mediated by many receptors that evoke Ca^{2+} signals (Morgado et al., 2012). This inhibition is assumed to be mediated by cAMP-dependent protein kinase (PKA) (Murthy, 2006), but there are also PKA-independent effects of cAMP (Spicuzza et al., 2001). At least some of these effects may be through exchange proteins activated by cAMP (EPACs), probably EPAC 1, which is abundant in blood vessels particularly within endothelial cells (Roscioni et al., 2011).

Histamine and prostaglandin E_2 (PGE_2) are two important inflammatory mediators. Their effects on VSM, which include regulation of proliferation (Yau and Zahradka, 2003) and vascular tone (Toda, 1987; Jadhav et al., 2004), are mediated by direct interactions with VSM and indirectly through release of autocrine signals from other cells (Norel, 2007). Histamine, PGE_2 and their receptors are also implicated in vascular pathology, including inflammation (Norel, 2007),

This work was supported by the Medical Research Council [G0900049], Biotechnology and Biological Sciences Research Council [L000075] and the Wellcome Trust [101844].
https://doi.org/10.1124/mol.117.109249.
[S] This article has supplemental material available at molpharm.aspetjournals.org.

ABBREVIATIONS: AC, adenylyl cyclase; AKAP, A kinase-anchoring protein; ASMC, aortic smooth muscle cell; $[Ca^{2+}]_i$, intracellular free $[Ca^{2+}]$; ci-IP_3, D-2,3-*O*-isopropylidene-6-*O*-(2-nitro-4,5-dimethoxy)benzyl-*myo*-inositol 1,4,5-trisphosphate; ci-IP_3PM, ci-IP3-hexakis(propionoxymethyl) ester; DDA, 2′,5′-dideoxyadenosine; EPAC, exchange protein activated by cAMP; ESI-09, 3-[5-(*tert*-butyl)isoxazol-3-yl]-2-[2-(3-chlorophenyl)hydrazono]-3-oxopropanenitrile; HBS, HEPES-buffered saline; HJC0197, 4-cyclopentyl-2-(2,5-dimethylbenzylsulfanyl)-6-oxo-1,6-dihydropyrimidine-5-carbonitrile; H89, *N*-[2-[[3-(4-bromophenyl)-2-propenyl]amino]ethyl]-5-isoquinolinesulfonamide dihydrochloride; IBMX, 3-isobutyl-1-methylxanthine; IP_3, inositol 1,4,5-trisphosphate; IP_3R, IP_3 receptor; L902, 688 (5-[(1*E*,3*R*)-4,4-difluoro-3-hydroxy-4-phenyl-1-buten-1-yl]-1-[6-(2*H*-tetrazol-5*R*-yl)hexyl]-2-pyrrolidinone); NKH 477, (*N*,*N*-dimethyl-(3*R*,4a*R*,5*S*,6a*S*,10*S*,10a*R*,10b*S*)-5-(acetyloxy)-3-ethenyldodecahydro-10,10b-dihydroxy-3,4a,7,7,10a-pentamethyl-1-oxo-1*H*-naphtho[2,1-*b*]pyran-6-yl ester β-alanine hydrochloride); PAR1, protease-activated receptor type 1; PDE, cyclic nucleotide phosphodiesterase; pIC_{50} (pEC_{50}), negative logarithm of the half-maximally inhibitory (effective) concentration; PGE_2, prostaglandin E_2; PKA, cAMP-dependent protein kinase; PKG, cGMP-dependent protein kinase; PKI (mut PKI), PKA inhibitor peptide (mutant inactive form); PLC, phospholipase C; SQ 22536, 9-(tetrahydro-2-furanyl)-9*H*-purin-6-amine; SQ/DDA, 1 mM SQ 22536 with 200 μM DDA; TBS, Tris-buffered saline; TBS-T, TBS with Tween; VASP, vasodilator-stimulated phosphoprotein; VSM, vascular smooth muscle.

atherosclerosis (Gómez-Hernández et al., 2006), and restenosis (Sasaguri et al., 2005).

We demonstrated previously that histamine, through H_1 receptors, stimulates an increase in $[Ca^{2+}]_i$ in human aortic smooth muscle cells (ASMC). The initial response is mediated by Ca^{2+} release through inositol 1,4,5-trisphosphate receptors (IP_3R) and it is followed by Ca^{2+} entry across the plasma membrane (Pantazaka et al., 2013). PGE_2, acting largely through EP_2 receptors, both stimulates the activity of adenylyl cyclase (AC) and substantially attenuates the Ca^{2+} signals evoked by histamine. Here, we show that inhibition of histamine-evoked Ca^{2+} signals by PGE_2 is mediated by cAMP delivered within "hyperactive signaling junctions." The response does not require EPACs, but it is attenuated by inhibition of PKA. The effect of PGE_2 on histamine-evoked Ca^{2+} signals does not result from a decrease in IP_3R sensitivity or from increased Ca^{2+} extrusion from the cytosol, nor does PGE_2 affect the Ca^{2+} signals evoked by stimulation of either endogenous type 1 protease-activated receptor (PAR1) or heterologously expressed muscarinic M3 acetylcholine receptors. We suggest that PKA uncouples H_1 histamine receptors from the guanine nucleotide-binding protein, $G_{q/11}$, and activation of phospholipase C (PLC). Our results establish that digital signaling from PGE_2 receptors, through cAMP and PKA, inhibits histamine-evoked Ca^{2+} signals.

Materials and Methods

Materials. H89, NKH 477, 8-Br-cAMP, and 8-Br-cGMP were from R&D Systems (Abingdon, Oxford, UK). *S*p-cAMPS, 6-Bnz-cAMP, 8-pCPT-2′-O-Me-cAMP, *R*p-cAMPS, *R*p-8-CPT-cAMPS, ESI-09, and HJC0197 were from Biolog (Bremen, Germany). Ionomycin, SQ 22536, DDA and myristoylated-PKA inhibitor peptide (PKI) were from Merck-Millipore (Watford, UK). A membrane-permeant peptide inhibitor of A kinase-anchoring proteins (AKAPs) [stearated Ht31 AKAP inhibitor peptide (st-Ht31)] and its proline-modified inactive form (st-Ht31P) were from Promega (Southampton, UK). Thapsigargin was from Alomone Laboratories (Jerusalem, Israel). PAR1 peptide, histamine dihydrochloride, forskolin, IBMX, and PGE_2 were from Sigma-Aldrich (Welwyn Garden City, UK). Butaprost (free acid) and L902,688 were from Cayman Chemicals (Ann Arbor, MI). Membrane-permeant caged IP_3 (ci-IP_3PM) was from SiChem (Bremen, Germany). [2,8-^{3}H] adenine ci-IP_3PM, D-2,3-O-isopropylidene-6-O-(2-nitro-4,5-dimethoxy)benzyl-myo-inositol 1,4,5-trisphosphate-hexakis(propionoxymethyl) ester was from Perkin Elmer (Seer Green, Bucks, UK). Fluo-8 was from Stratech Scientific Ltd (Newmarket, Suffolk, UK). Other reagents were from Sigma-Aldrich, sources specified previously (Pantazaka et al., 2013) or identified in this section.

Culture of Human Aortic Smooth Muscle Cells. Human ASMC from the American Tissue Culture Collection (Manassas, VA) or Dr. Trevor Littlewood (Boyle et al., 2002) were cultured as described (Pantazaka et al., 2013). Ethical approval for the latter was obtained from Addenbrooke's NHS Trust. Cells were derived from four Caucasian patients (males aged 23, 52, and 54, and a female aged 58), who died of causes unrelated to cardiovascular pathologies. Cells were used between passages two and six.

Measurements of $[Ca^{2+}]_i$. Histamine-evoked changes in $[Ca^{2+}]_i$ were recorded from cell populations using confluent cultures of ASMC grown in 96-well plates and loaded with Fluo-4 or Fluo-8. Experiments were performed in HEPES-buffered saline (HBS) at 20°C. HBS had the following composition (mM): NaCl 135, KCl 5.9, $MgCl_2$ 1.2, $CaCl_2$ 1.5, glucose 11.5, and HEPES 11.6 (pH 7.3). Fluorescence was recorded using a FlexStation 3 fluorescence plate-reader (MDS Analytical Technologies, Wokingham, UK) and calibrated to $[Ca^{2+}]_i$ as described (Pantazaka et al., 2013).

For measurements of $[Ca^{2+}]_i$ in single cells, confluent cultures of ASMC grown on poly-L-lysine-coated coverslips (22-mm diameter) were loaded with Fura-2 in HBS containing Fura-2 AM (4 μM), probenecid (2.5 mM), and pluronic F127 (0.02% v/v) for 1 hour at 20°C. Fluorescence (detected at >510 nm with alternating excitation at 340 and 380 nm) was recorded using an Olympus IX71 inverted fluorescence microscope and Luca (electron-multiplying charge-coupled device) EMCCD Andor Technology, Belfast, UK camera. After correction for background fluorescence, determined by addition of ionomycin (1–5 μM) in HBS containing $MnCl_2$ (1 mM), fluorescence ratios (F_{340}/F_{380}) were calibrated to $[Ca^{2+}]_i$ (Tovey et al., 2003).

Measurements of Intracellular cAMP. Confluent cultures of ASMC grown in 24-well plates and labeled with ^{3}H-adenine were incubated under conditions that replicated those used for measurements of $[Ca^{2+}]_i$. Reactions were terminated by aspiration of medium and addition of ice-cold trichloroacetic acid (5% v/v, 1 ml). After 30 minutes on ice, ^{3}H-cAMP was separated from other ^{3}H-labeled adenine nucleotides (Pantazaka et al., 2013).

Expression of PKI and M3 Muscarinic Receptors. Plasmids encoding PKI (pRSV-PKI-v2) and its inactive form (pRSV-mut PKI-v2) were from Addgene (cat. no. 45066 and cat. no. 45067; Cambridge, MA) (Day et al., 1989); they were C-terminally tagged with mCherry. Plasmid encoding the human M3 muscarinic acetylcholine receptor was from the cDNA Resource Centre (cat. no. MAR0300000) (Ford et al., 2002). The three constructs were each recombined into BacMam pCMV-DEST. Bacmids were then prepared, and virus was produced from bacmid-infected Sf9 cells according to the manufacturer's instructions (Thermo Fisher Scientific, Runcorn, UK). ASMC were infected at a multiplicity of infection (MOI) of ~50 and used after 96 hours.

Flash Photolysis of Caged IP_3. Confluent cultures of ASMC grown on poly-L-lysine-coated imaging dishes (35-mm diameter with a 7-mm glass insert; MatTek Corporation, Ashland, MA) were loaded (45 minutes, 20°C) with a membrane-permeant form of caged IP_3 (ci-IP_3PM, 1 μM) in HBS with probenecid (2.5 mM) and pluronic F127 (0.02% v/v). Fluo-4 AM (4 μM) was then added and after 45 minutes at 20°C, the medium was replaced with HBS containing only probenecid. After a further 45 minutes, this medium was replaced with HBS. Cells were illuminated with a 488-nm diode-based solid-state laser, and emitted fluorescence (500–550 nm) was captured with an EMCCD camera. Three UV flashes (each ~1-millisecond duration; <345 nm, 3000 μF, 300 V, ~170 J) from a JML-C2 Xe flash-lamp (Rapp OptoElectronic, Hamburg, Germany) allowed photolysis of caged IP_3 (ci-IP_3). Responses are reported as F/F_0, where F_0 and F are fluorescence intensities corrected for background recorded from the same region of interest immediately before (F_0) and after stimulation (F).

Measurements of IP_3 and PLC Activity. ASMC in 12-well plates were cultured until confluent. The medium was then supplemented with D-*myo*-[2-^{3}H]-inositol (10 μCi/ml) for 48 hours at 37°C. After washing, cells were incubated at 20°C in HBS with LiCl (10 mM) for 5 minutes before stimulation. Reactions were terminated by aspirating medium and adding cold $HClO_4$ (1 ml, 0.6 M) containing phytic acid (0.2 mg/ml). After 30 minutes, the acid-extract was removed, the cells were scraped into 50 mM Tris at pH 7 (400 μl), and the pooled extract and cells were centrifuged (10,000*g*, 2 minutes, 4°C). The supernatant was neutralized using K_2CO_3 (1 M) with EDTA (5 mM). ^{3}H-inositol phosphates were separated using ion-exchange columns.

For assays of IP_3 mass, ASMC in 75-cm^2 flasks were stimulated, the medium was removed, and the incubations were terminated by scraping cells into ice-cold ethanol (1 ml). After 30 minutes, extracts were dried and suspended in 300 μl of Tris-EDTA medium (TEM: 50 mM Tris, 1 mM EDTA, pH 8.3). Equilibrium-competition binding using ^{3}H-IP_3 (4.5 nM, 19.3 Ci/mmol), rat cerebellar membranes (10 μg) and cell extract (20–100 μl) in a final volume of 200 μl of TEM was used to determine the IP_3 content of the extracts (Rossi et al., 2009).

Immunoblotting. Confluent ASMC in 75-cm^2 flasks or six-well plates were stimulated and then scraped into cold phosphate-buffered saline supplemented with Triton-X-100 (1% w/v), protease inhibitors (one mini-tablet per 10 ml; Roche Applied Science, Burgess Hill, UK), and phosphatase inhibitors (10 μl/ml; Sigma-Aldrich). Scraped cells were disrupted by ~30 passages through a 28-gauge needle and sonicated (3 × 10 seconds). Proteins were separated by SDS-PAGE (NuPAGE 4%–12% Bis-Tris gels; Invitrogen, Paisley, UK) and transferred to a polyvinylidene difluoride membrane (iBlot; Invitrogen). Membranes were washed (5 minutes) with Tris-buffered saline (TBS: 137 mM NaCl, 20 mM Tris, pH 7.6), blocked by incubation in TBS containing 0.1% Tween-20 (TBS-T) and 5% (w/v) nonfat milk powder (1 hour, 20°C), and then washed with TBS-T (3 × 5 minutes). Blots were incubated for 12 hours at 4°C with primary antibody (1:1000) in TBS-T with 5% (w/v) BSA. After washing (3 × 5 minutes), blots were incubated with horseradish peroxidase-conjugated donkey anti-rabbit secondary antibody (1:2000; Santa Cruz Biotechnology, Dallas, TX) for 1 hour in TBS-T with 5% (w/v) nonfat milk powder. After further washing (3 × 5 minutes), bands were detected using ECL Prime (GE Healthcare, Chalfont St Giles, UK) and quantified using GeneTools (Syngene, Cambridge, UK). The primary rabbit antibodies recognize PKA-phosphorylated sequences RXXS*/T* (AbP1, AbP2, cat. nos. 9621 and 9624; New England Biolabs, Hitchin, UK; * denotes the phosphorylated residue) and vasodilator-stimulated phosphoprotein (VASP [clone 43, BD Biosciences, San Jose, CA]) phosphorylated at Ser-157 (New England Biolabs) or VASP clone 43 (BD Biosciences, San Jose, CA).

Quantitative PCR Analysis. QPCR was performed as described (Tovey et al., 2008) using primers specific for AC subtypes (Ludwig and Seuwen, 2002) and calibrated against expression of the housekeeping gene, glyceraldehyde 3-phosphate dehydrogenase (GAPDH) (Pantazaka et al., 2013). Human BioBank cDNA pooled from a variety of tissues (Primerdesign, Southampton, UK) was used as a positive control for AC subtypes not expressed in ASMC.

Statistical Analysis. Concentration-effect relationships were individually fitted by nonlinear curve-fitting to Hill equations (GraphPad Prism, La Jolla, CA). The absolute sensitivities and amplitudes of the responses to histamine and PGE_2 varied between patients and with cell passage. Results are, therefore, often presented as normalized values (e.g., as percentages of a maximal response) or as differences between paired comparisons (e.g., ΔpIC_{50}). Two-tailed paired or unpaired Student's t test, or one-way analysis of variance followed by Bonferroni's test, were used as appropriate.

Results

Cyclic AMP Mediates Inhibition of Histamine-Evoked Ca^{2+} Signals by PGE_2. Figure 1A demonstrates that PGE_2 inhibits the Ca^{2+} signals evoked by histamine in human ASMC. Most experiments were performed at 20°C to minimize loss of the cytosolic Ca^{2+} indicator. However, in parallel analyses we confirmed that a maximally effective concentration of PGE_2 (10 μM) caused indistinguishable inhibition of the Ca^{2+} signals evoked by histamine (100 μM) whether the analyses were performed at 20°C (47% ± 12% inhibition, n = 4) or 37°C (45% ± 6%). In parallel measurements of the effects of PGE_2 on intracellular cAMP and histamine-evoked Ca^{2+} signals, the cAMP response [negative logarithm of the half-maximally effective concentration (pEC_{50}) = 6.76 ± 0.09, n = 4) was ~140-fold less sensitive to PGE_2 than were the Ca^{2+} signals [negative logarithm of the half-maximally inhibitory concentration (pIC_{50}) = 8.90 ± 0.10, n = 6] (Fig. 1B). This relationship is consistent with PGE_2 evoking formation of more cAMP than needed to maximally inhibit Ca^{2+} signals, and with cAMP lying upstream of the inhibition of Ca^{2+} signaling (Strickland and Loeb, 1981).

Forskolin and its water-soluble analog, NKH 477, directly activate eight of the nine membrane-bound forms of AC (AC1–8) (Seifert et al., 2012). Pretreatment of ASMC with NKH 477 caused a concentration-dependent reduction in both the peak amplitudes of the Ca^{2+} signals evoked by histamine and their sensitivity to histamine (Fig. 1C; Table 1). Similar results were obtained with forskolin (Fig. 1D). Maximally effective concentrations of PGE_2 and NKH 477 caused indistinguishable inhibition of histamine-evoked Ca^{2+} signals, and their combined maximal effects were not additive (Fig. 1E). These results are consistent with reports showing that forskolin and NKH 477 attenuate the Ca^{2+} signals evoked by receptors, including H_1 receptors that stimulate PLC in VSM (Yang et al., 1999, and references therein) and other smooth muscles. There has, however, been no prior demonstration that activation of AC inhibits PLC-evoked Ca^{2+} signals in human ASMC.

High concentrations of 8-Br-cAMP also inhibited histamine-evoked Ca^{2+} signals by reducing the maximal response and the sensitivity to histamine (Fig. 2A). 8-Br-cAMP had no effect on the Ca^{2+} content of the intracellular stores (Fig. 2B). The effects of 8-Br-cAMP were mimicked by *S*p-cAMPS, which activates PKA and EPACs, and by 6-Bnz-cAMP and 8-CPT-6-Phe-cAMP, which activate PKA but not EPACs (Fig. 2C; Supplemental Fig. S1; and Table 1). A high concentration (10 mM) of 8-pCPT-2′-O-Me-cAMP, a membrane-permeant activator of EPACs; and *R*p-cAMPS and *R*p-8-CPT-cAMPS, antagonists of both PKA and EPACs, were ineffective (Fig. 2D; Supplemental Fig. S1).

The negative result with 8-pCPT-2′-O-Me-cAMP is important because this analog is more membrane-permeable than 8-Br-cAMP, and it both binds with greater affinity than cAMP to EPACs and more effectively activates them (Gloerich and Bos, 2010). Furthermore, antagonists of EPACs 1 and 2, HJC0197 (Chen et al., 2012), and ESI-09 (Almahariq et al., 2013) (10 μM, 20 minutes) did not prevent the inhibition of histamine-evoked Ca^{2+} signals by PGE_2 (Fig. 2E). Higher concentrations (50 μM) of either antagonist abolished the Ca^{2+} signals evoked by histamine (data not shown). We have not explored this effect further, although the antagonists caused similar inhibition of carbachol-evoked Ca^{2+} signals in human embryonic kidney 293 cells (Meena et al., 2015). Others have also reported nonspecific effects of these EPAC antagonists (Rehmann, 2013).

Maximally effective concentrations of PGE_2, forskolin, NKH 477, or 8-Br-cAMP similarly attenuated the Ca^{2+} signals evoked by histamine, and combinations of the treatments were not additive (Fig. 2D). These results establish that inhibition of histamine-evoked Ca^{2+} signals by PGE_2 is mediated by cAMP (Fig. 2F) and does not require EPACs.

Inhibition of Histamine-Evoked Ca^{2+} Signals by PGE_2 is Not Mediated by cGMP-Dependent Protein Kinase. Cyclic AMP may directly activate PKG in arterial smooth muscle, although this is contentious [see references in Morgan et al. (2014)]. Cyclic AMP could, however, increase the concentration of cGMP by competing with it for degradation by cyclic nucleotide phosphodiesterases (PDEs). Stimulation of PKG might then attenuate IP_3-evoked Ca^{2+} release (Masuda et al., 2010). There is evidence, however, that expression of

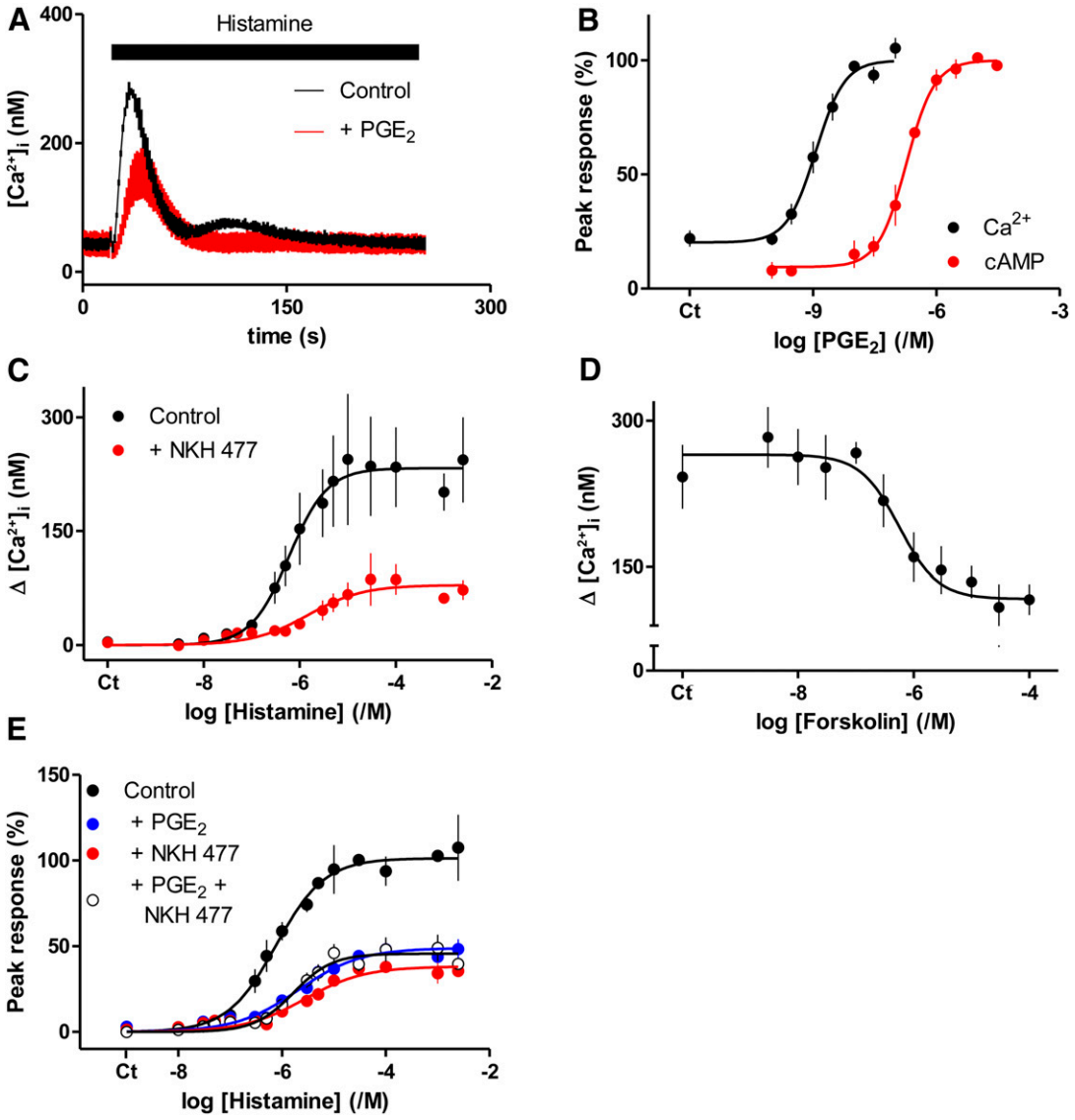

Fig. 1. Inhibition of histamine-evoked Ca^{2+} signals by PGE_2 is mediated by cAMP. (A) Ca^{2+} signals evoked by histamine (3 μM, black bar) alone or with PGE_2 (10 μM, added 5 minutes before and then during stimulation with histamine). Results show means ± range from two wells on a single plate; they are typical of results from at least four independent experiments. (B) Effects of PGE_2 on cAMP accumulation (measured after 5 minutes) and inhibition of the peak Ca^{2+} signals evoked by histamine (3 μM). Results, as percentages of maximal inhibition (Ca^{2+}) or stimulation (cAMP), are means ± S.E.M. from six and four experiments, respectively. This panel includes some data for cAMP measurements that were published previously (Pantazaka et al., 2013). (C) Effect of NKH 477 (100 μM) on the peak Ca^{2+} signal evoked by histamine. (D) Concentration-dependent effects of forskolin on the peak Ca^{2+} signals evoked by histamine (1 mM). (E) Effect of PGE_2 (10 μM), NKH 477 (100 μM), or both on the peak Ca^{2+} signals evoked by histamine (as percentages of the maximal response). NKH 477, forskolin, or PGE_2 were added 5 minutes before and then during stimulation with histamine. Results show means ± S.E.M. from four (C and D) or three (E) independent plates with one to three wells analyzed from each. Ct denotes control.

proteins involved in PKG signaling in VSM are downregulated in culture (Lincoln et al., 2006, and references therein). 8-Br-cGMP (pIC_{50} = 4.50 ± 0.29, n = 5) partially inhibited Ca^{2+} signals evoked by a submaximal concentration of histamine, but the maximal inhibition was less than half that evoked by PGE_2 or 8-Br-cAMP (Fig. 3, A and B). Furthermore, and in contrast to the effects of 8-Br-cAMP (Fig. 2C), 8-Br-cGMP did not inhibit the Ca^{2+} signals evoked by a maximal histamine concentration (Fig. 2D). Prolonged incubation with IBMX (20 minutes, 1 mM), a nonselective inhibitor of PDEs, inhibited histamine-evoked Ca^{2+} signals, but the inhibition (33% ± 3%, n = 4) was less than that caused by PGE_2 (56% ± 3%) (Fig. 3C). More importantly, a maximal concentration of PGE_2 similarly inhibited histamine-evoked Ca^{2+} signals in

TABLE 1

Inhibition of histamine-evoked Ca^{2+} signals by PGE_2 and cAMP

Cells were incubated for the times shown with the indicated drugs before recording the peak increase in $[Ca^{2+}]_i$ evoked by histamine (3 μM; 1 mM for forskolin and NKH 477). Results (means ± S.E.M. from n independent experiments) show the maximal inhibition of the histamine-evoked Ca^{2+} signals and the pIC_{50} for each drug.

	pIC_{50}	Maximal inhibition	n
	/M	%	
PGE_2 (5 min)	9.01 ± 0.05	64 ± 4	9
Butaprost (5 min)	7.28 ± 0.09	61 ± 1	6
L902,688 (5 min)	9.35 ± 0.10	76 ± 4	5
8-Br-cAMP (20 min)	2.98 ± 0.20	85 ± 3	3
6-Bnz-cAMP (20 min)	3.73 ± 0.14	64 ± 5	5
Forskolin (5 min)	6.24 ± 0.11	57 ± 6	4
NKH 477 (5 min)	5.50 ± 0.18	53 ± 4	5

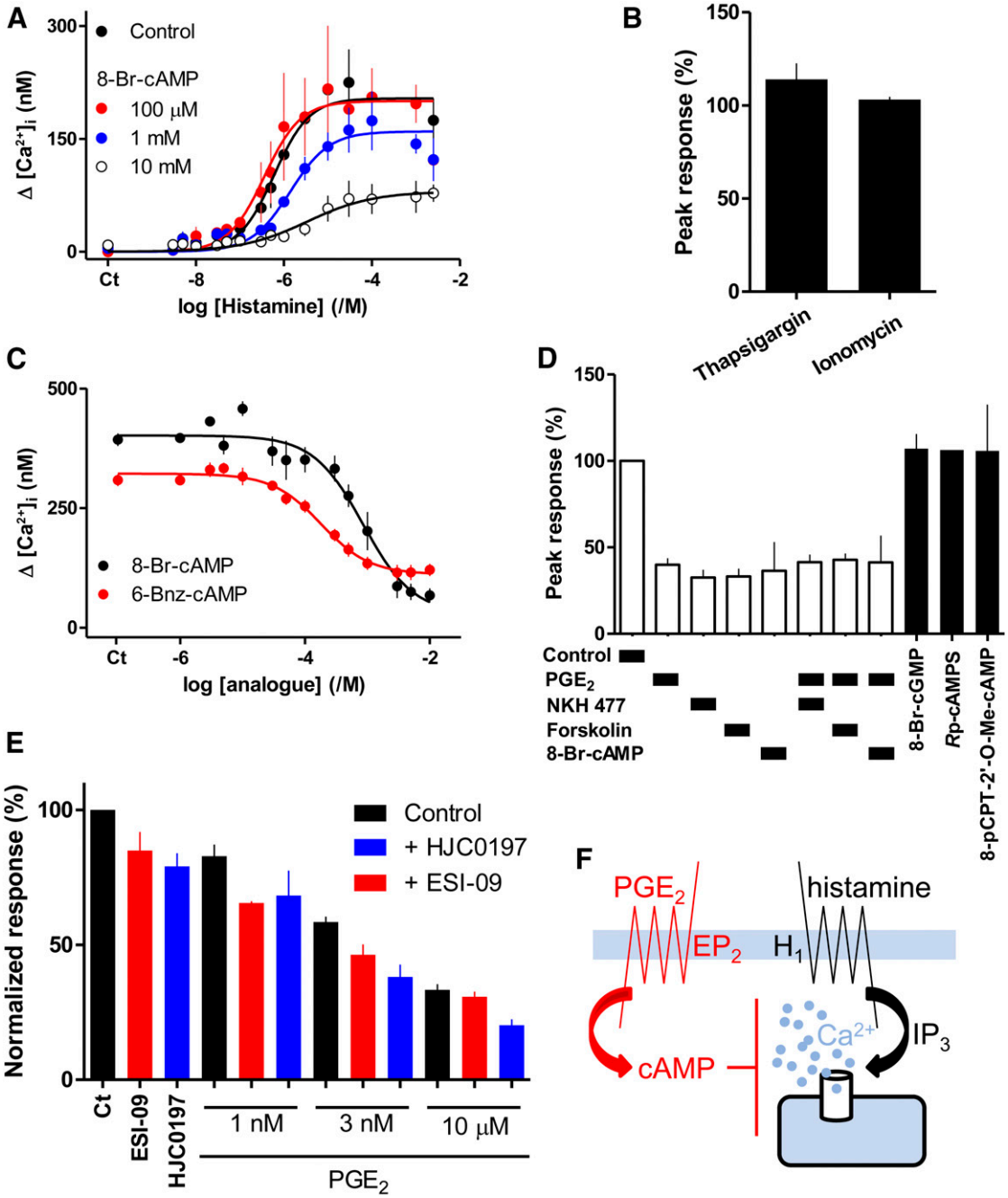

Fig. 2. Cyclic AMP mediates inhibition of histamine-evoked Ca^{2+} signals by PGE_2. (A) Effect of 8-Br-cAMP (added 20 minutes before histamine) on the peak Ca^{2+} signals evoked by the indicated concentrations of histamine. Results are means ± S.E.M. from at least three experiments with one to three wells in each. (B) 8-Br-cAMP (10 mM, 20 minutes) had no effect on the Ca^{2+} content of the intracellular stores as revealed by the increases in $[Ca^{2+}]_i$ evoked by addition of thapsigargin (1 μM) or ionomycin (1 μM) in Ca^{2+}-free HBS. Results (percentages of responses without 8-Br-cAMP) are means ± S.E.M. from five experiments with three to four wells analyzed in each. (C) Effect of the indicated cyclic nucleotides (added 20 minutes before histamine) on the peak Ca^{2+} signals evoked by histamine (3 μM). Results are means ± S.E.M. from three to five experiments with two to three wells in each. (D) Effect of NKH 477 (100 μM, 5 minutes), forskolin (100 μM, 5 minutes), 8-Br-cAMP (10 mM, 20 minutes), PGE_2 (10 μM, 5 minutes), 8-Br-cGMP (10 mM, 20 minutes), *Rp*-cAMPS (10 mM, 20 minutes), or 8-pCPT-2′-O-Me-cAMP (10 mM, 20 minutes) alone or in combination on the peak Ca^{2+} signals evoked by histamine (1 mM). Results (as percentages of the response to histamine alone) are means ± S.E.M. from three experiments with two to three wells in each. Results for *Rp*-cAMPS are from a single experiment with three replicates, limited by the availability of this expensive analog. (E) Effects of the EPAC antagonists, ESI-09 and HJC0197 (10 μM, 20 minutes), on the Ca^{2+} signals evoked by histamine (3 μM) added 5 minutes before and then during treatment with the indicated concentrations of PGE_2. Results are expressed as percentages of the paired response to histamine alone (means ± S.E.M., $n = 3–5$; $n = 2$ for the antagonists with 1 and 3 nM PGE_2, where error bars show ranges). (F) The results establish that cAMP mediates inhibition of histamine-evoked Ca^{2+} signals by PGE_2.

the presence and absence of IBMX (Fig. 3C), demonstrating that the effects of PGE_2 are not mediated by inhibition of PDEs. We conclude that inhibition of histamine-evoked Ca^{2+} signals by PGE_2 is not mediated by inhibition of PDEs and consequent accumulation of cGMP.

Histamine and 8-Br-cAMP Stimulate PKA-Mediated Protein Phosphorylation in Different Microenvironments. Most effects of cAMP are mediated by PKA, EPACs, or cyclic nucleotide-regulated plasma membrane cation channels (Gloerich and Bos, 2010; Cooper and Tabbasum, 2014).

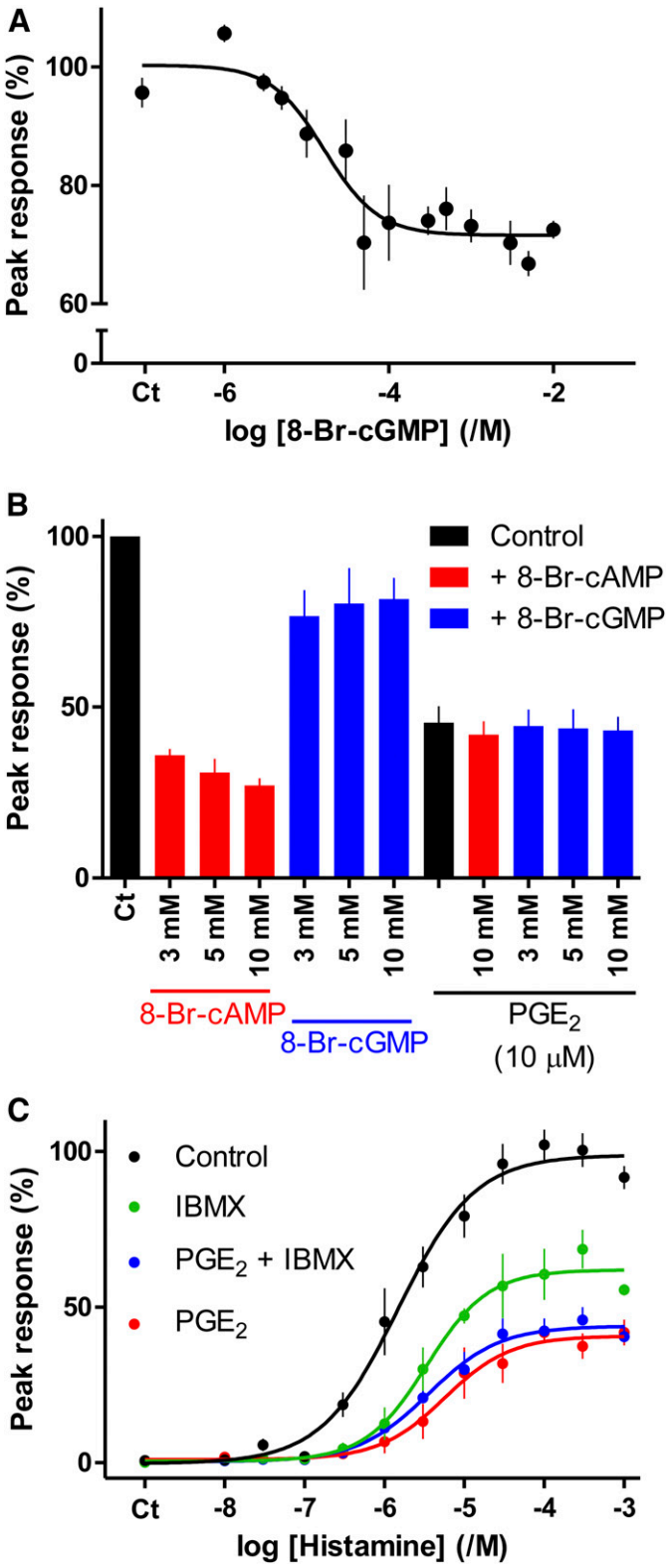

Fig. 3. Inhibition of histamine-evoked Ca^{2+} signals by PGE_2 is not mediated by cGMP. (A) Concentration-dependent effects of 8-Br-cGMP (20 minutes) on the peak Ca^{2+} signals evoked by histamine (3 μM). (B) Similar experiments show the responses to histamine (3 μM) after preincubation with PGE_2 (10 μM, 5 minutes) and/or the indicated concentrations of 8-Br-cAMP or 8-Br-cGMP (20 minutes). (C) Peak Ca^{2+} signals evoked by histamine alone or after incubation with IBMX (1 mM, 20 minutes), PGE_2 (10 μM, 5 minutes), or both. Results (as percentages of response to histamine alone) are means ± S.E.M. from five (A), three to six (B; n = 2 for 3 and 5 mM 8-Br-cAMP, where ranges are shown), and four to seven (C) independent experiments with two to three wells in each.

The latter cannot mediate the effects of cAMP on IP_3-evoked Ca^{2+} release, nor are EPACs responsible. We therefore assessed the role of PKA.

Immunoblotting with an antiserum that recognizes sequences phosphorylated by PKA showed that maximally effective concentrations of PGE_2 or 8-Br-cAMP stimulated similar levels of protein phosphorylation in ASMC and their effects were nonadditive (Fig. 4A). The phosphorylation was mimicked by 6-Bnz-cAMP but not by the EPAC-selective analog 8-pCPT-2′-O-Me-cAMP (Fig. 4A). PGE_2-evoked protein phosphorylation was attenuated by inhibition of either PKA (with H89) or AC [with 1 mM SQ 22536 with 200 μM DDA (SQ/DDA)] (Fig. 4B).

Maximal concentrations of PGE_2 and 8-Br-cAMP caused phosphorylation of the same proteins (Fig. 4A), but the two stimuli differed in their susceptibility to PKA inhibitors. *R*p-8-CPT-cAMPS, an inhibitor of PKA that competes with cAMP by binding to the regulatory subunit of PKA, abolished the phosphorylation evoked by 8-Br-cAMP but only partially inhibited that evoked by PGE_2 (Fig. 4C). Conversely, H89, which inhibits PKA (and other kinases) by competing for the ATP-binding site, abolished the phosphorylation evoked by PGE_2 but caused lesser inhibition of the response to 8-Br-cAMP (Fig. 4C). Similar results were obtained when an antiserum to phospho-VASP was used to assess PKA-mediated phosphorylation (Supplemental Fig. S2).

These results suggest that PKA activated by PGE_2 may be exposed to high local concentrations of cAMP, which might then effectively compete with the inhibitor *R*p-8-CPT-cAMPS. Conversely, PKA activated by 8-Br-cAMP, which would probably be uniformly distributed within the cell, may be more accessible to ATP than PKA activated by PGE_2, and so less susceptible to inhibition by H89.

Inhibition of Histamine-Evoked Ca^{2+} Signals by PGE_2 Is Attenuated by Inhibition of PKA. Inhibition of histamine-evoked Ca^{2+} signals by PGE_2 or 8-Br-cAMP was inhibited by *R*p-8-CPT-cAMPS (1 mM), which reduced the sensitivity to PGE_2 (decreasing the pIC_{50} for PGE_2 from 8.68 ± 0.17 to 8.26 ± 0.05, n = 3; ΔpIC_{50} = 0.4 ± 0.1, where $\Delta pIC_{50} = pIC_{50}^{control} - pIC_{50}^{Rp\text{-}8\text{-}CPT\text{-}cAMPS}$) and 8-Br-cAMP ($\Delta pIC_{50}$ = 0.6 ± 0.1) without affecting the maximal inhibition (Fig. 5, A and B). These results are consistent with *R*p-8-CPT-cAMPS competitively inhibiting cAMP binding to PKA and thereby attenuating the effects of cAMP on Ca^{2+} signals.

H89 (10 μM) also attenuated the inhibition of histamine-evoked Ca^{2+} signals by 8-Br-cAMP (ΔpIC_{50} = 1.13 ± 0.18 n = 3) and PGE_2 (Fig. 5, A and B). In keeping with our analyses of protein phosphorylation (Fig. 4C), the inhibition of histamine-evoked Ca^{2+} signals by maximal concentrations of PGE_2 were less effectively inhibited by H89 than were the effects of maximal concentrations of 8-Br-cAMP (compare Fig. 5, A and B).

PKI inhibits PKA by competing with its peptide substrates. We could not achieve effective inhibition of PKA-mediated protein phosphorylation with myristoylated-PKI (10 μM, 20 minutes, data not shown). But using a baculovirus, we achieved expression of PKI in >90% of cells, and this caused 49% ± 6% (n = 3) inhibition of the VASP phosphorylation evoked by PGE_2 (100 nM) (Supplemental Fig. S3). Expression of an inactive PKI (mut PKI) had no effect on PGE_2-evoked protein phosphorylation (Supplemental Fig. S3). The effects of H89 and PKI on the inhibition of histamine-evoked

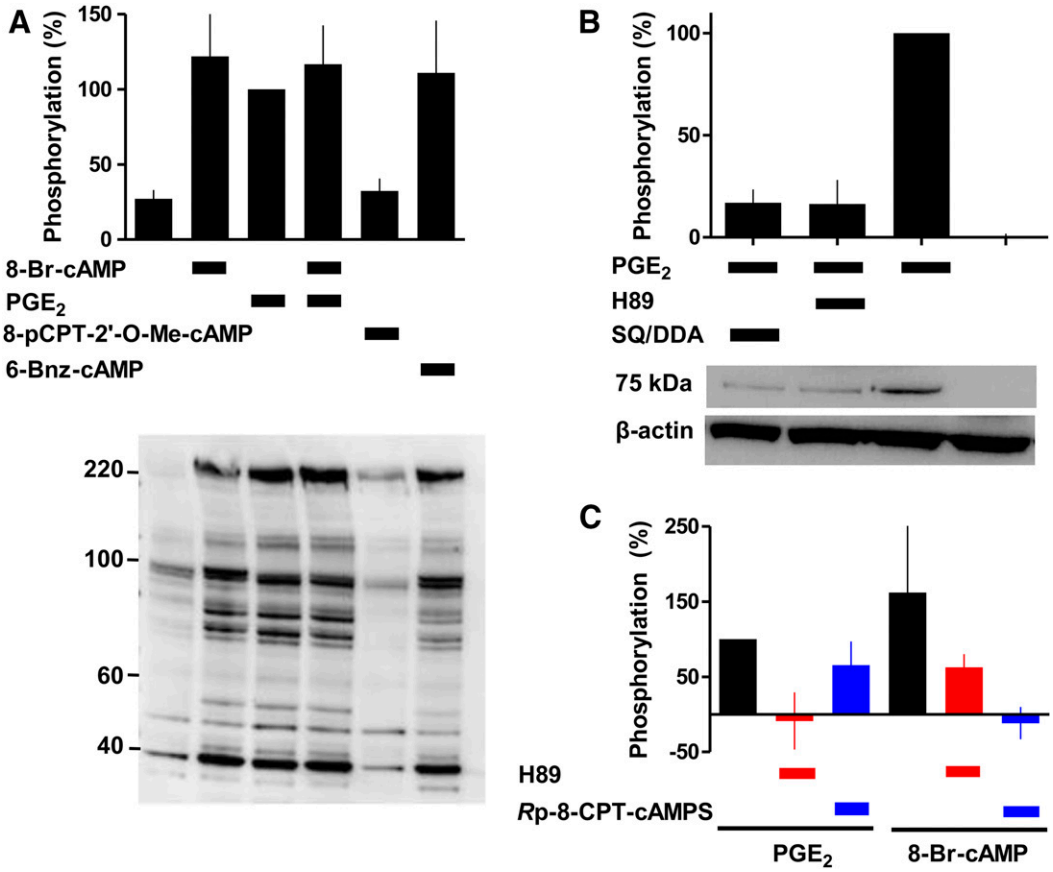

Fig. 4. PGE_2 and 8-Br-cAMP stimulate PKA-mediated protein phosphorylation. (A) Typical immunoblot using AbP2 (see *Materials and Methods*) showing PKA-phosphorylated proteins from cells stimulated with cAMP analogs (10 mM, 20 minutes) or PGE_2 (10 μM, 5 minutes). Summary results (means ± S.D., n = 3–4) show the band intensity across the entire gel as a percentage of that from cells stimulated with PGE_2. M_r markers (kilodaltons) shown alongside gel. (B) Similar analyses using AbP1 show the effects of H89 (10 μM, 10 minutes) or SQ/DDA (1 mM SQ22536 and 200 μM DDA, 20 minutes) on the phosphorylation of a 75-kDa band in response to PGE_2 (10 μM. 5 minutes). Summary results (means ± S.D., n = 3–5) show band intensities as percentages of the matched response to PGE_2 alone. (C) Similar analysis to (A), for cells stimulated with PGE_2 (10 μM, 5 minutes) or 8-Br-cAMP (10 mM, 20 minutes) alone or after incubation (20 minutes) with *R*p-8-CPT-cAMPS (1 mM) H89 (10 μM). Results (means ± S.D., n = 3–4) show the increase in phosphorylation evoked by the indicated stimuli expressed as a percentage of the matched response to PGE_2 alone.

Ca^{2+} signals by PGE_2 were similar: Each substantially reduced the maximal inhibition without significantly affecting the IC_{50} for PGE_2 (Fig. 5, A and C). The effects of H89 on inhibition of histamine-evoked Ca^{2+} signals by selective agonists of EP_2 (butaprost) and EP_4 (L902,688) receptors were similar to those observed with PGE_2 (Supplemental Fig. S4). We conclude that inhibition of histamine-evoked Ca^{2+} signals by PGE_2 is mediated by cAMP and requires PKA (Fig. 5D).

PGE_2 Does Not Inhibit Ca^{2+} Release Evoked by Direct Activation of IP_3Rs. The rate at which $[Ca^{2+}]_i$ recovered from the peak Ca^{2+} signal evoked by histamine was unaffected by PGE_2 (half-times for recovery were 19 ± 1 and 17 ± 1 seconds, after histamine alone or with PGE_2, respectively; n = 11) (Supplemental Fig. S5). This suggests that the attenuated Ca^{2+} signals do not result from PGE_2 stimulating Ca^{2+} extrusion from the cytosol.

We used flash-photolysis of ci-IP_3 to activate IP_3R directly in Fluo-4-loaded ASMC. Single-cell analyses of ASMC established that most cells (99% ± 1%, from 12 fields) responded to histamine (1 mM) with an increase in $[Ca^{2+}]_i$, and that two successive challenges with histamine evoked indistinguishable Ca^{2+} signals (Fig. 6, A and B). PGE_2 reduced the peak amplitude of the Ca^{2+} signal evoked by a second histamine challenge by 28% ± 4% (n = 65 cells), without significantly affecting the number of cells that responded (91% ± 8% and 83% ± 7% for control and PGE_2-treated cells, respectively) (Fig. 6, C and D). These results confirm that under the conditions used for uncaging ci-IP_3, PGE_2 inhibits histamine-evoked Ca^{2+} signals.

ASMC loaded with ci-IP_3 responded to UV flashes with rapid increases in Fluo-4 fluorescence (F/F_0, see *Materials and Methods*). The amplitudes of these signals were less than those evoked by a maximal concentration of histamine (Fig. 6, E and F), confirming that responses to photolysis of ci-IP_3 were not saturated. Although cells responded similarly to successive histamine challenges (Fig. 6, A and B), the response to a second photolysis of ci-IP_3 was smaller than the first (Fig. 6G), presumably because each stimulus depleted a fraction of the ci-IP_3. We therefore used two methods to assess the effects of PGE_2 on the Ca^{2+} signals evoked by photolysis of ci-IP_3. Cells were either stimulated twice with a UV stimulus, and the amplitude of the second response (with or without PGE_2) was compared with the first response for each cell (R2/R1) (Fig. 6, G–I), or cells were stimulated once with UV flashes alone or in the presence of PGE_2 (Fig. 6J). Both analyses concur in demonstrating that PGE_2 has no significant effect on the Ca^{2+} signals evoked by IP_3 (Fig. 6, G–J). The results with ci-IP_3 therefore demonstrate that PGE_2 does not affect the

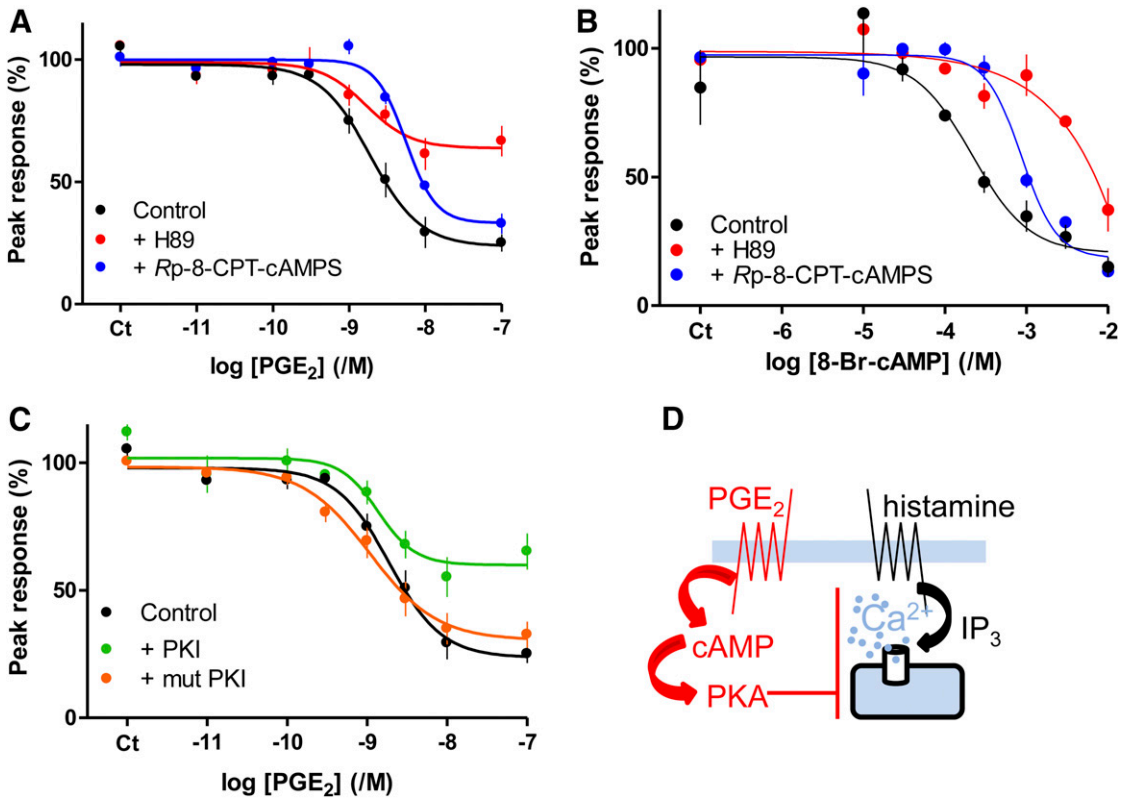

Fig. 5. Inhibition of histamine-evoked Ca^{2+} signals by PGE_2 or 8-Br-cAMP requires PKA. (A and B) Effects of PGE_2 (5 minutes) or 8-Br-cAMP (20 minutes) on the peak Ca^{2+} signals evoked by histamine (3 μM) alone or with H89 (10 μM, 20 minutes) or *R*p-8-CPT-cAMPS (1 mM, 20 minutes). (C) Effects of PGE_2 (5 minutes) on the Ca^{2+} signals evoked by histamine (3 μM) in cells infected with baculovirus expressing PKI or its inactive form (mut PKI). Results (A–C) are means ± S.E.M. from three experiments with two to three wells in each. (D) The results suggest that PKA mediates the inhibition of histamine-evoked Ca^{2+} signals by PGE_2.

interactions of IP_3 with IP_3R. Furthermore, because the peak IP_3-evoked Ca^{2+} signals were unaffected by PGE_2 under conditions where it attenuates responses to histamine (Fig. 6, I and J), the results provide additional evidence that PGE_2 does not stimulate Ca^{2+} removal from the cytosol.

The product of ci-IP_3 photolysis is an active but modified form of IP_3 (D-2,3-*O*-isopropylidene-*myo*-inositol 1,4,5-trisphosphate) (Dakin and Li, 2007) that is not a substrate for IP_3 3-kinase and may differ from IP_3 in its rate of dephosphorylation. Our results do not therefore exclude the possibility that PGE_2 may accelerate degradation of IP_3. These results suggest that PGE_2 attenuates histamine-evoked Ca^{2+} signals by inhibiting IP_3 formation, stimulating IP_3 degradation, and/or disrupting IP_3 delivery to IP_3Rs.

PGE_2 Attenuates Histamine-Evoked Accumulation of IP_3. Using an assay that reports PLC activity (stimulation after blocking inositol monophosphate degradation by Li^+), histamine (1 mM, 30 minutes) stimulated a small accumulation of ^{3}H-inositol phosphates in ASMC. Although the response was modestly attenuated by PGE_2 (10 μM), the effect was not statistically significant (Fig. 7A). Using an IP_3R-based bioassay that detects only (1,4,5)IP_3, histamine stimulated IP_3 accumulation, and the response was attenuated by PGE_2, although the latter again failed to achieve statistical significance (Fig. 7B). We also attempted to measure histamine-evoked IP_3 formation in single cells using a fluorescence resonance energy transfer (FRET)-based IP_3 sensor (Gulyas et al., 2015), but the signals were too small to resolve reliably any inhibitory effect of PGE_2. Available genetically encoded IP_3 sensors are known to have limited dynamic range and limited capacity to resolve small changes in intracellular IP_3 concentration (Miyamoto and Mikoshiba, 2017).

We assessed the responses of ASMC to other stimuli (ATP, bradykinin, carbachol, phenylephrine, and thrombin) that might be expected to evoked Ca^{2+} signals through receptors that stimulate Gq (results not shown). Only thrombin reproducibly evoked substantial increases in $[Ca^{2+}]_i$. Thrombin is a protease that cleaves the type 1 protease-activated receptor (PAR1) to unmask an N-terminal ligand. Thrombin and the PAR1 peptide itself evoked concentration-dependent increases in $[Ca^{2+}]_i$ in ASMC (Fig. 7C). In parallel analyses, PGE_2 (10 μM, 5 minutes) attenuated the Ca^{2+} signals evoked by histamine without affecting those evoked by PAR1 peptide (Fig. 7D). Although the maximal increase in $[Ca^{2+}]_i$ evoked by PAR1 peptide was larger than that evoked by histamine, with concentrations of histamine and the PAR1 peptide that evoked comparable increases in $[Ca^{2+}]_i$, only the response to histamine was inhibited by PGE_2 (Fig. 7E). After heterologous expression of human muscarinic M3 acetylcholine receptors in ASMC, carbachol evoked a concentration-dependent (pEC_{50} = 7.72 ± 0.04, n = 3) increase in $[Ca^{2+}]_i$, with a maximal increase (272 ± 31 nM, n = 3) comparable to that evoked by histamine (204 ± 13 nM, Fig. 2A). However, the responses to carbachol were unaffected by PGE_2 (Fig. 7F). These results, demonstrating that PGE_2 selectively inhibits the Ca^{2+} signals evoked by histamine, suggest that the inhibition probably does not arise downstream of PLC.

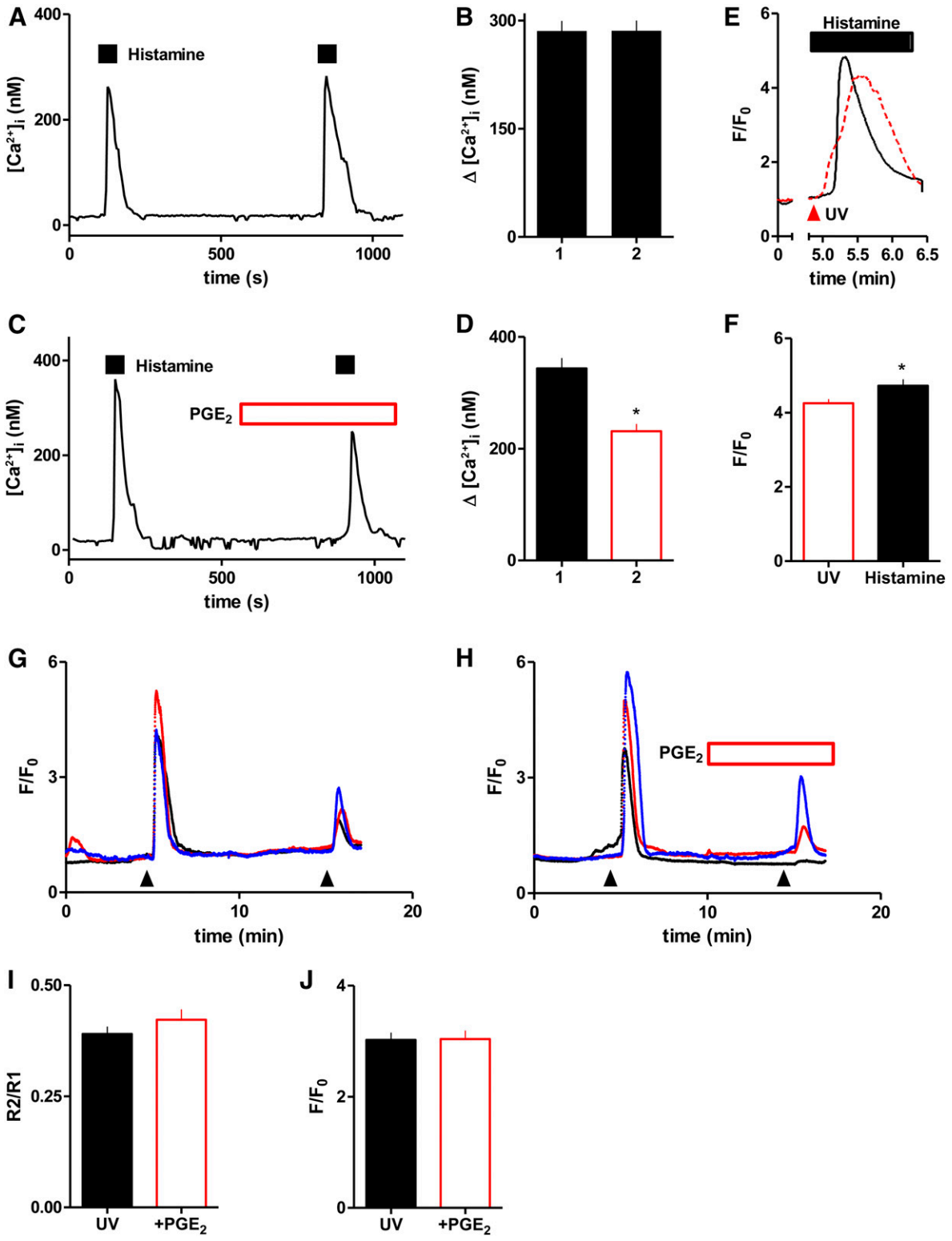

Fig. 6. PGE_2 does not inhibit Ca^{2+} signals evoked by direct activation of IP_3 receptors. (A–D) Typical fluorescence traces from single Fura-2-loaded ASMC sequentially stimulated with histamine (1 mM) alone (A) or with PGE_2 (10 μM) (C). Summary results (means ± S.E.M., 65 cells from six independent fields) show peak amplitudes of the first and second responses to histamine in the absence (B) or presence (D) of PGE_2. (E) Typical fluorescence traces from single Fluo-4-loaded ASMC stimulated with a UV flash to photolyse ci-IP_3 (red trace) or histamine (1 mM, black trace). (F) Summary results (means ± S.E.M. from 35 and 118 cells, for histamine and ci-IP_3 respectively) show peak responses. (G and H) Three typical fluorescence traces from single ASMC stimulated twice with UV flashes (arrowheads) alone (G) or with PGE_2 (10 μM) (H). (I) Summary results (means ± S.E.M. from 50–68 cells) show relative amplitudes of the peak responses (R2/R1). (J) Summary results (means ± S.E.M. from 36–43 cells) show F/F_0 (see *Materials and Methods*) for cells stimulated with a UV flash alone or with PGE_2 (10 μM added 5 minutes before flash). *$P < 0.05$, relative to the response to histamine alone (D, paired Student's t test) or to the UV flash alone (F, unpaired Student's t test).

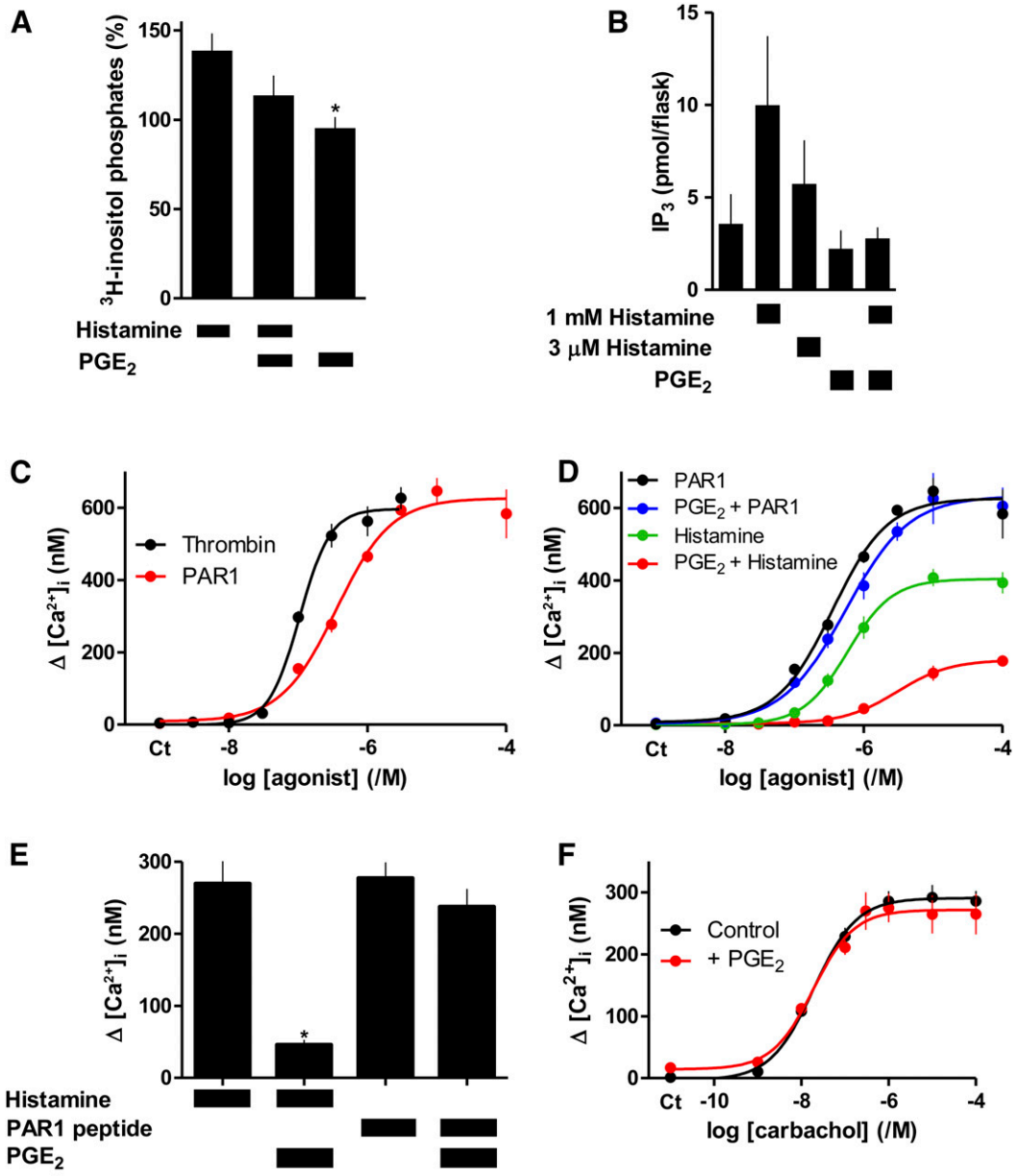

Fig. 7. PGE_2 selectively attenuates activation of PLC by histamine. (A) Accumulation of ^{3}H-inositol phosphates (30 minutes) in cells incubated with LiCl and stimulated with histamine (1 mM) alone or with PGE_2 (10 μM). Results are shown as percentages of matched analyses from unstimulated cells. (B) Mass assays of (1,4,5)IP_3 from cells treated with histamine (1 minute) alone or after treatment with PGE_2 (10 μM, 5 minutes). Results (A and B) are means ± S.E.M., n = 3–5, *$P < 0.05$, relative to 1 mM histamine, one-way analysis of variance with Bonferroni's test. (C) Peak Ca^{2+} signals evoked by the indicated concentrations of thrombin or PAR1 peptide. (D) Effects of PGE_2 (10 μM, 5 minutes) on the peak Ca^{2+} signals evoked by the indicated concentrations of histamine or PAR1 peptide. Results (C and D) are means ± S.E.M., n = 4–5. (E) Comparison of the effects of PGE_2 on Ca^{2+} signals of similar amplitude evoked by histamine or PAR1 peptide. (F) Peak increases in $[Ca^{2+}]_i$ in ASMC heterologously expressing M3 muscarinic receptors and stimulated in Ca^{2+}-free HBS with the indicated concentrations of carbachol alone or with PGE_2 (10 μM, 5 minutes). Results are means ± S.E.M., n = 3, with six replicates for each. There was no response to carbachol in normal ASMC (data not shown).

Histamine-Evoked Ca^{2+} Signals Are Inhibited by Local cAMP Signals. Inhibitors of AC (SQ/DDA) attenuated PGE_2-evoked cAMP formation (by 79% ± 2%, n = 4) (Fig. 8A) and protein phosphorylation (Fig. 4B). However, SQ/DDA had no effect on the inhibition of histamine-evoked Ca^{2+} signals evoked by PGE_2 or butaprost (Fig. 8, B and C). Although cAMP mediates the inhibition of Ca^{2+} signals by PGE_2, the response to a maximal concentration of PGE_2 might survive substantial inhibition of AC because it stimulates formation of more cAMP than needed to maximally inhibit Ca^{2+} signals (Fig. 1B). However, the same argument cannot account for the lack of effect of SQ/DDA on responses to submaximal concentrations of PGE_2. How might a submaximal response to PGE_2 be unaffected by substantial inhibition of cAMP formation and PKA activity (Fig. 4B; Fig. 8, A and B)?

A possible explanation is that SQ 22356 and DDA, related inhibitors that bind to the ATP-binding site of AC (Brand et al., 2013), selectively inhibit subtypes of AC distinct from those that mediate the effects of PGE_2. Available antibodies do not allow quantitative assessment of the expression of AC

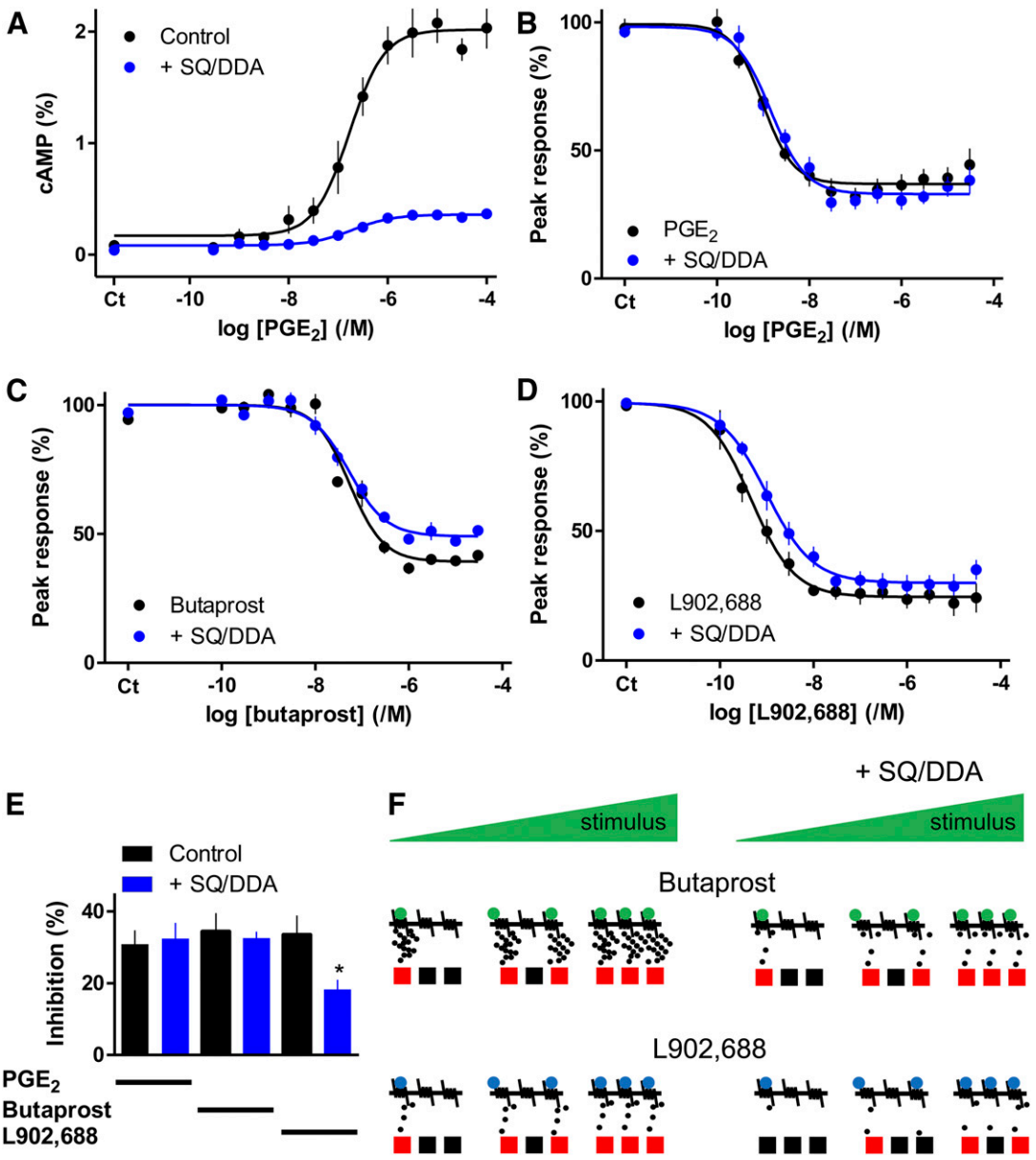

Fig. 8. Signaling from EP receptors to Ca^{2+} signals via cAMP junctions. (A) Concentration-dependent effects of PGE_2 on intracellular cAMP (5 minutes) alone or after treatment with SQ/DDA (20 minutes). Results [cAMP/(ATP + ADP + cAMP), %] are means ± S.E.M. from four experiments [three of these were published in Pantazaka et al. (2013)]. (B–D) Concentration-dependent effects of PGE_2, butaprost, or L902,688 on the Ca^{2+} signals evoked by histamine (3 μM) in the presence of SQ/DDA (20 minutes). Results are means ± S.E.M. from nine (B), six (C), or five (D) experiments with two to three wells in each. (E) Summary data show the effects of SQ/DDA on the inhibition of histamine-evoked Ca^{2+} signals by concentrations of PGE_2 (1 nM), butaprost (30 nM), and L902,688 (0.3 nM) that approximately match their IC_{50} values. (F) Junctional delivery of cAMP to the PKA (squares) through which it inhibits (red) histamine-evoked Ca^{2+} signals. Activation of EP_2 or EP_4 receptors with butaprost or L902,688, respectively, inhibits histamine-evoked Ca^{2+} signals, but the latter evokes formation of less cAMP. We propose, from our results with SQ/DDA, that cAMP is locally delivered to PKA within each signaling junction at a concentration more than sufficient to cause a maximal effect. The concentration-dependent inhibition of Ca^{2+} signals by prostanoids is proposed to result from recruitment of all-or-nothing cAMP signaling junctions, rather than from graded increases in activity within individual junctions. EP_2 receptors deliver more cAMP than EP_4 receptors and are therefore more resistant to inhibition of AC by SQ/DDA. Hence inhibition of Ca^{2+} signals by EP_4 receptors is partially inhibited by SQ/DDA, whereas the response to EP_2 receptors is insensitive (right). *$P < 0.05$, paired Student's t-test relative to control.

subtypes, but QPCR analysis shows that human ASMC express similar amounts (~30%) of AC3, AC7, AC9, some AC6 (~10%), and detectable AC4 (~2%) (Supplemental Fig. S6). AC9 probably does not mediate the effects of PGE_2 on Ca^{2+} signals because AC9 is insensitive to forskolin and NKH 477 (Seifert et al., 2012), which mimic the effects of PGE_2 on Ca^{2+} signals (Fig. 1, C–E; Fig. 2D). Among the remaining ACs expressed in ASMC, SQ22536 and DDA probably have some selectivity for AC6 over AC3 and AC7 despite some inconsistent reports (Pierre et al., 2009; Seifert et al., 2012). From analyses of individual AC isoforms, maximally effective concentrations of SQ 22356 (and other P-site inhibitors) inhibit catalytic activity by only ~80% [Brand et al. (2013), but see Onda et al. (2001)]. This is similar to the ~80% inhibition of PGE_2-evoked cAMP accumulation by SQ/DDA in ASMC (Fig. 8A), suggesting that the incomplete inhibition observed in ASMC probably does not reflect the unperturbed activity of SQ/DDA-insensitive ACs. Furthermore, the effects

of PGE_2 on protein phosphorylation in ASMC are inhibited by SQ/DDA (Fig. 4B), again suggesting that the ACs activated by PGE_2 are inhibited. We conclude that the lack of effect of SQ/DDA on PGE_2-mediated inhibition of histamine-evoked Ca^{2+} signals is probably not the result of ineffective inhibition of an SQ/DDA-resistant subtype of AC.

To account for the results with SQ/DDA, we suggest that cAMP is delivered locally to PKA at concentrations more than sufficient to fully inhibit Ca^{2+} signals. The concentration-dependent effects of PGE_2 might then result from recruitment of these "hyperactive" cAMP signaling junctions, rather than from increased activity within individual junctions (Fig. 8F). This interpretation is consistent with analyses of the effects of SQ/DDA on the inhibition of Ca^{2+} signals by selective activation of EP_4 receptors. Although activation of EP_2 and EP_4 receptors causes similar maximal inhibition of histamine-evoked Ca^{2+} signals, EP_4 receptors cause less stimulation of AC (Pantazaka et al., 2013). This suggests that EP_4 receptors may less effectively saturate the cAMP signaling junctions. Whereas inhibition of AC with SQ/DDA had no effect on the inhibition of histamine-evoked Ca^{2+} signals by PGE_2 or butaprost (to selectively activate EP_2 receptors), the sensitivity to L902,688, a selective agonist of EP_4 receptors, was modestly reduced by SQ/DDA ($\Delta pIC_{50} = 0.32 \pm 0.10$, $n = 5$) (Fig. 8, B–E). This observation supports our suggestion that the subtype(s) of AC that link prostanoid receptors to inhibition of Ca^{2+} signals are sensitive to SQ/DDA. Furthermore, these results are consistent with the scheme shown in Fig. 8F, where we suggest that cAMP is locally delivered within "hyperactive" signaling junctions at concentrations more than sufficient to maximally activate the PKA that inhibits Ca^{2+} signals.

We considered whether AKAPs, which are widely implicated in assembling PKA with its regulators and effectors (Smith et al., 2017), might contribute to organization of the cAMP signaling through PKA that leads to inhibition of histamine-evoked Ca^{2+} signals. A membrane-permeant peptide that disrupts association of AKAPs with PKA (st-Ht31) but not its inactive analog (st-Ht31P), significantly attenuated the protein phosphorylation evoked by PGE_2, but neither peptide affected the concentration-dependent inhibition of histamine-evoked Ca^{2+} signals by PGE_2 (Supplemental Fig. S7). These results suggest that AKAPs are probably not important components of the signaling pathway from PGE_2 to inhibition of Ca^{2+} signals.

Discussion

In human ASMC, the IP_3-mediated Ca^{2+} signals evoked by activation of H_1 histamine receptors are attenuated by PGE_2. Several lines of evidence show that this inhibition is mediated by cAMP. The concentration-effect relationships for regulation of AC and Ca^{2+} signals by PGE_2 are consistent with cAMP lying upstream of Ca^{2+} in the signaling pathway (Fig. 1B), direct activation of AC or membrane-permeant analogs of cAMP mimic PGE_2, and maximal concentrations of these drugs are not additive (Figs. 1 and 2). Our conclusion that cAMP mediates the inhibition of Ca^{2+} signals in human ASMC is consistent with evidence that many receptors, via stimulation of AC, attenuate Ca^{2+} signaling in smooth muscle, including VSM (Morgado et al., 2012). Inhibition of histamine-evoked Ca^{2+} signals by PGE_2 does not require activation of EPACs (Fig. 2, D and E). The inhibition is not mediated by accumulation of cGMP after inhibition of PDEs since neither cGMP nor inhibition of PDEs effectively mimicked PGE_2 (Fig. 3). Inhibition of histamine-evoked Ca^{2+} signals by PGE_2 or 8-Br-cAMP was attenuated by inhibition of PKA using H89, PKI, or *R*p-8-CPT-cAMPS (Fig. 4). We conclude that inhibition of histamine-evoked Ca^{2+} signals by PGE_2 is (at least largely) mediated by PKA (Fig. 5D).

PKA can enhance Ca^{2+} removal from the cytosol by stimulating Ca^{2+} pumps (Tada and Toyofuku, 1998) or the Na^+/Ca^{2+} exchanger (Karashima et al., 2007). However, accelerated removal of cytosolic Ca^{2+} does not mediate inhibition of histamine-evoked Ca^{2+} signals by PGE_2 in human ASMC (Supplemental Fig. S5). Nor would this mechanism be consistent with the lack of effect of PGE_2 on the Ca^{2+} signals evoked by stimulation of endogenous PAR1 or heterologously expressed M3 muscarinic receptors (Fig. 7, D–F). Cyclic AMP has been proposed to inhibit IP_3-evoked Ca^{2+} release (Bai and Sanderson, 2006), but PKA (IP_3R1 and IP_3R2) and cAMP (IP_3R1-3) more often potentiate responses to IP_3 (Taylor, 2017). However, under conditions where PGE_2 inhibited histamine-evoked Ca^{2+} signals, it had no effect on the sensitivity of IP_3Rs to IP_3 (Fig. 6). Steps linking receptors to PLC can also be inhibited by cAMP (see references in Yang et al. (1999)). Although two different assays suggested that PGE_2 attenuated histamine-evoked PLC activity in human ASMC, neither analysis demonstrated a statistically significant effect (Fig. 7, A and B). However, the lack of effect of PGE_2 on the Ca^{2+} signals evoked by PAR1 and muscarinic M3 receptors (Fig. 7, D–F) suggests that the inhibition of histamine-evoked Ca^{2+} signals by cAMP/PKA is probably the result of uncoupling of H_1 histamine receptors from $G_{q/11}$. PKA has been reported to phosphorylate H_1 histamine receptors (Kawakami et al., 2003; Horio et al., 2004), but the functional consequences have not been thoroughly examined (Miyoshi et al., 2006). We conclude that in human ASMC, PGE_2, through EP_2 and EP_4 receptors (Pantazaka et al., 2013), stimulates AC, leading to formation of cAMP and uncoupling of histamine from stimulation of PLC, most probably by PKA-mediated phosphorylation of H_1 receptors.

Cyclic AMP can be locally delivered to intracellular targets (Zaccolo, 2011; Cooper and Tabbasum, 2014). AKAPs play prominent roles in targeting cAMP through PKA to specific cellular responses (Smith et al., 2017), but our results suggest that AKAPs probably do not contribute to inhibition of histamine-evoked Ca^{2+} signals by PGE_2 (Supplemental Fig. S7). Our results do, however, reveal an additional complexity in the pathways linking PGE_2 to inhibition of histamine-evoked Ca^{2+} signals. Although cAMP mediates this inhibition, the concentration-dependent effects of PGE_2 were insensitive to substantial inhibition of AC (Fig. 8). These results and analyses of the effects of selective activation of EP_2 and EP_4 receptors lead to the scheme shown in Fig. 8F. We suggest that communication between EP receptors and the PKA that inhibits histamine-evoked IP_3 formation is mediated by delivery of cAMP within signaling junctions. Activation of a junction allows local delivery of a supersaturating concentration of cAMP to PKA, allowing each junction to function as a robust on-off switch. We suggest that the concentration-dependent effects of PGE_2 arise from recruitment of these junctions and not from graded activity within individual junctions. Such digital

signaling from receptors to intracellular targets via hyperactive junctions (Fig. 8F) allows robust and reliable communication, and may be a general feature of signaling by diffusible intracellular messengers (Tovey et al., 2008).

Acknowledgments

The authors thank Trevor Littlewood (Department of Biochemistry, University of Cambridge, UK) for ASMC and Peter Varnai (Department of Physiology, Semmelweis University, Hungary) for providing the FRET IP_3 sensor. The authors also thank Stephen Tovey for discussions and Sriram Govindan for preliminary analyses (Department of Pharmacology, University of Cambridge, UK).

Authorship Contributions

Participated in research design: E. Taylor, Pantazaka, C. Taylor.
Conducted experiments: E. Taylor, Pantazaka, Shelley.
Performed data analysis: E. Taylor, Pantazaka, Shelley, C. Taylor.
Wrote or contributed to the writing of the manuscript: E. Taylor, Pantazaka, Shelley, C. Taylor.

References

Almahariq M, Tsalkova T, Mei FC, Chen H, Zhou J, Sastry SK, Schwede F, and Cheng X (2013) A novel EPAC-specific inhibitor suppresses pancreatic cancer cell migration and invasion. *Mol Pharmacol* **83**:122–128.
Bai Y and Sanderson MJ (2006) Airway smooth muscle relaxation results from a reduction in the frequency of Ca^{2+} oscillations induced by a cAMP-mediated inhibition of the IP_3 receptor. *Respir Res* **7**:34.
Boyle JJ, Weissberg PL, and Bennett MR (2002) Human macrophage-induced vascular smooth muscle cell apoptosis requires NO enhancement of Fas/Fas-L interactions. *Arterioscler Thromb Vasc Biol* **22**:1624–1630.
Brand CS, Hocker HJ, Gorfe AA, Cavasotto CN, and Dessauer CW (2013) Isoform selectivity of adenylyl cyclase inhibitors: characterization of known and novel compounds. *J Pharmacol Exp Ther* **347**:265–275.
Chen H, Tsalkova T, Mei FC, Hu Y, Cheng X, and Zhou J (2012) 5-Cyano-6-oxo-1,6-dihydro-pyrimidines as potent antagonists targeting exchange proteins directly activated by cAMP. *Bioorg Med Chem Lett* **22**:4038–4043.
Cooper DM and Tabbasum VG (2014) Adenylate cyclase-centred microdomains. *Biochem J* **462**:199–213.
Dakin K and Li WH (2007) Cell membrane permeable esters of D-*myo*-inositol 1,4,5-trisphosphate. *Cell Calcium* **42**:291–301.
Day RN, Walder JA, and Maurer RA (1989) A protein kinase inhibitor gene reduces both basal and multihormone-stimulated prolactin gene transcription. *J Biol Chem* **264**:431–436.
Ford DJ, Essex A, Spalding TA, Burstein ES, and Ellis J (2002) Homologous mutations near the junction of the sixth transmembrane domain and the third extracellular loop lead to constitutive activity and enhanced agonist affinity at all muscarinic receptor subtypes. *J Pharmacol Exp Ther* **300**:810–817.
Gloerich M and Bos JL (2010) Epac: defining a new mechanism for cAMP action. *Annu Rev Pharmacol Toxicol* **50**:355–375.
Gómez-Hernández A, Martín-Ventura JL, Sánchez-Galán E, Vidal C, Ortego M, Blanco-Colio LM, Ortega L, Tuñón J, and Egido J (2006) Overexpression of COX-2, prostaglandin E synthase-1 and prostaglandin E receptors in blood mononuclear cells and plaque of patients with carotid atherosclerosis: regulation by nuclear factor-kappaB. *Atherosclerosis* **187**:139–149.
Gulyás G, Tóth JT, Tóth DJ, Kurucz I, Hunyady L, Balla T, and Várnai P (2015) Measurement of inositol 1,4,5-trisphosphate in living cells using an improved set of resonance energy transfer-based biosensors. *PLoS One* **10**:e0125601.
Horio S, Ogawa M, Kawakami N, Fujimoto K, and Fukui H (2004) Identification of amino acid residues responsible for agonist-induced down-regulation of histamine H_1 receptors. *J Pharmacol Sci* **94**:410–419.
Jadhav V, Jabre A, Lin SZ, and Lee TJ (2004) EP_1- and EP_3-receptors mediate prostaglandin E_2-induced constriction of porcine large cerebral arteries. *J Cereb Blood Flow Metab* **24**:1305–1316.
Karashima E, Nishimura J, Iwamoto T, Hirano K, Hirano M, Kita S, Harada M, and Kanaide H (2007) Involvement of Na^+-Ca^{2+} exchanger in cAMP-mediated relaxation in mice aorta: evaluation using transgenic mice. *Br J Pharmacol* **150**:434–444.
Kawakami N, Miyoshi K, Horio S, Yoshimura Y, Yamauchi T, and Fukui H (2003) Direct phosphorylation of histamine H_1 receptor by various protein kinases in vitro. *Methods Find Exp Clin Pharmacol* **25**:685–693.
Lincoln TM, Wu X, Sellak H, Dey N, and Choi CS (2006) Regulation of vascular smooth muscle cell phenotype by cyclic GMP and cyclic GMP-dependent protein kinase. *Front Biosci* **11**:356–367.
Ludwig MG and Seuwen K (2002) Characterization of the human adenylyl cyclase gene family: cDNA, gene structure, and tissue distribution of the nine isoforms. *J Recept Signal Transduct Res* **22**:79–110.
Masuda W, Betzenhauser MJ, and Yule DI (2010) $InsP_3R$-associated cGMP kinase substrate determines inositol 1,4,5-trisphosphate receptor susceptibility to phosphoregulation by cyclic nucleotide-dependent kinases. *J Biol Chem* **285**:37927–37938.
Meena A, Tovey SC, and Taylor CW (2015) Sustained signalling by PTH modulates IP_3 accumulation and IP_3 receptors through cyclic AMP junctions. *J Cell Sci* **128**:408–420.
Miyamoto A and Mikoshiba K (2017) Probes for manipulating and monitoring IP_3. *Cell Calcium* **64**:57–64.
Miyoshi K, Das AK, Fujimoto K, Horio S, and Fukui H (2006) Recent advances in molecular pharmacology of the histamine systems: regulation of histamine H_1 receptor signaling by changing its expression level. *J Pharmacol Sci* **101**:3–6.
Morgado M, Cairrão E, Santos-Silva AJ, and Verde I (2012) Cyclic nucleotide-dependent relaxation pathways in vascular smooth muscle. *Cell Mol Life Sci* **69**:247–266.
Morgan SJ, Deshpande DA, Tiegs BC, Misior AM, Yan H, Hershfeld AV, Rich TC, Panettieri RA, An SS, and Penn RB (2014) β-Agonist-mediated relaxation of airway smooth muscle is protein kinase A-dependent. *J Biol Chem* **289**:23065–23074.
Murthy KS (2006) Signaling for contraction and relaxation in smooth muscle of the gut. *Annu Rev Physiol* **68**:345–374.
Norel X (2007) Prostanoid receptors in the human vascular wall. *Sci World J* **7**:1359–1374.
Onda T, Hashimoto Y, Nagai M, Kuramochi H, Saito S, Yamazaki H, Toya Y, Sakai I, Homcy CJ, Nishikawa K, et al. (2001) Type-specific regulation of adenylyl cyclase. Selective pharmacological stimulation and inhibition of adenylyl cyclase isoforms. *J Biol Chem* **276**:47785–47793.
Pantazaka E, Taylor EJA, Bernard WG, and Taylor CW (2013) Ca^{2+} signals evoked by histamine H_1 receptors are attenuated by activation of prostaglandin EP_2 and EP_4 receptors in human aortic smooth muscle cells. *Br J Pharmacol* **169**:1624–1634.
Pierre S, Eschenhagen T, Geisslinger G, and Scholich K (2009) Capturing adenylyl cyclases as potential drug targets. *Nat Rev Drug Discov* **8**:321–335.
Rehmann H (2013) Epac-inhibitors: facts and artefacts. *Sci Rep* **3**:3032.
Roscioni SS, Maarsingh H, Elzinga CR, Schuur J, Menzen M, Halayko AJ, Meurs H, and Schmidt M (2011) Epac as a novel effector of airway smooth muscle relaxation. *J Cell Mol Med* **15**:1551–1563.
Rossi AM, Riley AM, Tovey SC, Rahman T, Dellis O, Taylor EJA, Veresov VG, Potter BVL, and Taylor CW (2009) Synthetic partial agonists reveal key steps in IP_3 receptor activation. *Nat Chem Biol* **5**:631–639.
Sasaguri Y, Wang KY, Tanimoto A, Tsutsui M, Ueno H, Murata Y, Kohno Y, Yamada S, and Ohtsu H (2005) Role of histamine produced by bone marrow-derived vascular cells in pathogenesis of atherosclerosis. *Circ Res* **96**:974–981.
Seifert R, Lushington GH, Mou TC, Gille A, and Sprang SR (2012) Inhibitors of membranous adenylyl cyclases. *Trends Pharmacol Sci* **33**:64–78.
Smith FD, Esseltine JL, Nygren PJ, Veesler D, Byrne DP, Vonderach M, Strashnov I, Eyers CE, Eyers PA, Langeberg LK, et al. (2017) Local protein kinase A action proceeds through intact holoenzymes. *Science* **356**:1288–1293.
Spicuzza L, Belvisi MG, Birrell MA, Barnes PJ, Hele DJ, and Giembycz MA (2001) Evidence that the anti-spasmogenic effect of the beta-adrenoceptor agonist, isoprenaline, on guinea-pig trachealis is not mediated by cyclic AMP-dependent protein kinase. *Br J Pharmacol* **133**:1201–1212.
Strickland S and Loeb JN (1981) Obligatory separation of hormone binding and biological response curves in systems dependent upon secondary mediators of hormone action. *Proc Natl Acad Sci USA* **78**:1366–1370.
Tada M and Toyofuku T (1998) Molecular regulation of phospholamban function and expression. *Trends Cardiovasc Med* **8**:330–340.
Taylor CW (2017) Regulation of IP_3 receptors by cyclic AMP. *Cell Calcium* **63**:48–52.
Toda N (1987) Mechanism of histamine actions in human coronary arteries. *Circ Res* **61**:280–286.
Tovey SC, Dedos SG, Taylor EJA, Church JE, and Taylor CW (2008) Selective coupling of type 6 adenylyl cyclase with type 2 IP_3 receptors mediates direct sensitization of IP_3 receptors by cAMP. *J Cell Biol* **183**:297–311.
Tovey SC, Goraya TA, and Taylor CW (2003) Parathyroid hormone increases the sensitivity of inositol trisphosphate receptors by a mechanism that is independent of cyclic AMP. *Br J Pharmacol* **138**:81–90.
Yang CM, Chiu CT, Wang CC, Tsao HL, and Fan LW (1999) Forskolin inhibits 5-hydroxytryptamine-induced phosphoinositide hydrolysis and Ca^{2+} Mobilisation in canine cultured aorta smooth muscle cells. *Cell Signal* **11**:697–704.
Yau L and Zahradka P (2003) PGE_2 stimulates vascular smooth muscle cell proliferation via the EP_2 receptor. *Mol Cell Endocrinol* **203**:77–90.
Zaccolo M (2011) Spatial control of cAMP signalling in health and disease. *Curr Opin Pharmacol* **11**:649–655.

Address correspondence to: Dr. Colin W. Taylor, Department of Pharmacology, Tennis Court Road, Cambridge CB2 1PD, UK. E-mail: cwt1000@cam.ac.uk

Supplemental Materials

Prostaglandin E_2 Inhibits Histamine-Evoked Ca^{2+} Release in Human Aortic Smooth Muscle Cells through Hyperactive cAMP Signalling Junctions and Protein Kinase A

Emily J. A. Taylor, Evangelia Pantazaka, Kathryn L. Shelley and Colin W. Taylor

Department of Pharmacology, University of Cambridge, Cambridge, UK

Supplemental Table S1 Properties of the cyclic nucleotide analogues used. Data from Christensen *et al*. (2003), Poppe *et al*. (2008), Rehmann *et al*. (2003) and http://www.biolog.de. Where known, the lipophilicity of each analogue relative to cAMP is shown in parentheses. PKA binds cAMP with ~1000-fold greater affinity than does EPAC.

Analogue		Properties
8-Br-cAMP	8-bromo-adenosine-3′,5′-cyclic monophosphate	Similar affinity to cAMP for PKA, but ~10-fold greater affinity than cAMP for EPAC. Despite this selectivity, PKA is 100-fold more sensitive than EPAC to 8-Br-cAMP. More membrane-permeant than cAMP (***1.8***).
6-Bnz-cAMP	N^6-benzyladenosine-3′,5′-cyclic monophosphate	More membrane-permeant than 8-Br-cAMP. Relative affinity for binding to PKA and EPAC similar to cAMP (~1000-fold greater affinity for PKA), but scarcely activates EPAC. More selective, therefore, than cAMP in activating PKA (***6***).
*S*p-cAMPS	*S*p adenosine-3′,5′-cyclic monophosphorothioate	Low-affinity, PDE-resistant, activator of PKA. Also activates EPACs. (***1.3***).
*R*p-cAMPS	*R*p adenosine-3′,5′-cyclic monophosphorothioate	Competitive, low-affinity inhibitor of PKA. Very low-affinity activator of EPAC 1 (***1.3***).
*R*p-8-CPT-cAMPS	*R*p 8-(4-chlorophenylthio)-adenosine-3′,5′-cyclic monophosphorothioate	Most membrane-permeant inhibitor of PKA. Low-affinity antagonist of EPAC (***42***).
8-CPT-6-Phe-cAMP	8-(4-chlorophenylthio)-N^6-phenyladenosine-3', 5'-cyclic monophosphate	Membrane-permeant, PDE-resistant, selective and potent activator of PKA.
8-pCPT-2′-O-Me-cAMP (aka 007)	8-(4-chlorophenylthio)-2'-O-methyladenosine-3',5'-cyclic monophosphate	Activates EPAC, but not PKA. Greater affinity and efficacy for EPAC activation than cAMP (***70***).
ESI-09	3- [5-(tert-butyl)isoxazol-3-yl]-2-[2-(3-chlorophenyl)hydrazono]-3-oxopropanenitrile	Membrane-permeant selective inhibitor of EPACs 1 and 2. See text for discussion of off-target effects.
HJC0197	4-cyclopentyl-2-(2,5-dimethylbenzylsulfanyl)-6-oxo-1, 6-dihydropyrimidine-5-carbonitrile	Membrane-permeant selective inhibitor of EPACs 1 and 2.

Christensen AE, Selheim F, de Roooij J, Dremier S, Schwede F, Dao KK, Martinez A, Maenhaut C, Bos JL, GeniesermH.-G. and Døskeland SO (2003) cAMP analog mapping of epac1 and cAMP kinase. Discriminating analogs demonstrate that Epac and cAMP kinase act syneristically to promote PC12 cell neurite extension. *J Biol Chem* **278**:35394-35402.

Poppe H, Rybalkin SD, Rehmann H, Hinds TR, Tang XB, Christensen AE, Schwede F, Genieser HG, Bos JL, Doskeland SO, Beavo JA and Butt E (2008) Cyclic nucleotide analogs as probes of signaling pathways. *Nat Methods* **5**:277-278.

Rehmann H, Schwede F, Doskeland SO, Wittinghofer A and Bos JL (2003) Ligand-mediated activation of the cAMP-responsive guanine nucleotide exchange factor Epac. *J Biol Chem* **278**:38548-38556.

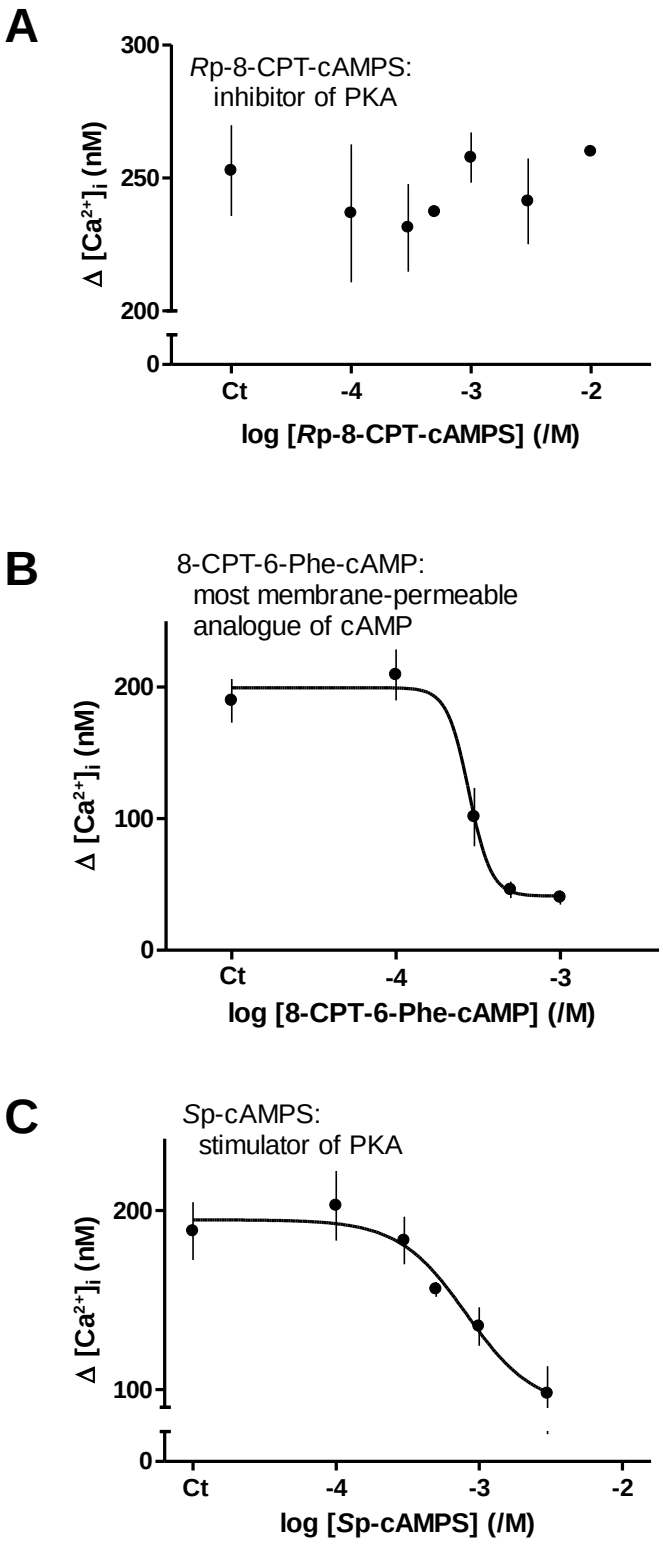

Supplemental Fig. S1. Effects of cAMP analogues on histamine-evoked Ca^{2+} signals. (A-C) Effects of the indicated concentrations of cyclic nucleotide analogues (20 min) on the peak Ca^{2+} signals evoked by histamine (1 mM). Results are from a single experiment with 2-3 replicates, limited by the availability of expensive analogues. Error bars show ranges for the replicate determinations.

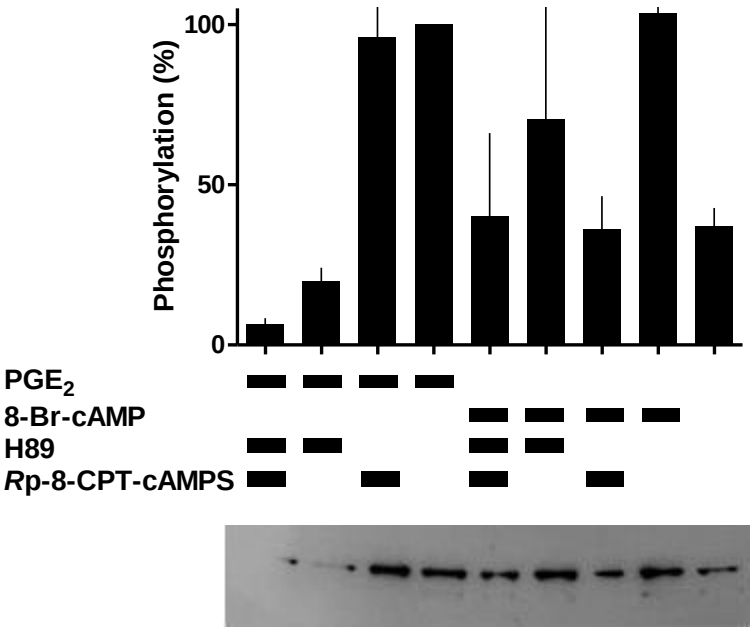

Supplemental Fig. S2. Effects of PGE_2 and 8-Br-cAMP on PKA-mediated phosphorylation of VASP in human ASMC. Cells were stimulated with PGE_2 (10 µM, 5 min) or 8-Br-cAMP (10 mM, 20 min) alone or after preincubation (20 min) with H89 (10 µM) or *R*p-8-CPT-cAMPS (1 mM). Results (means ± range, n = 2) show the intensity of the 50-kDa phospho-VASP band as a percentage of that for cells stimulated with PGE_2. One of the two immunoblots is shown beneath the graph.

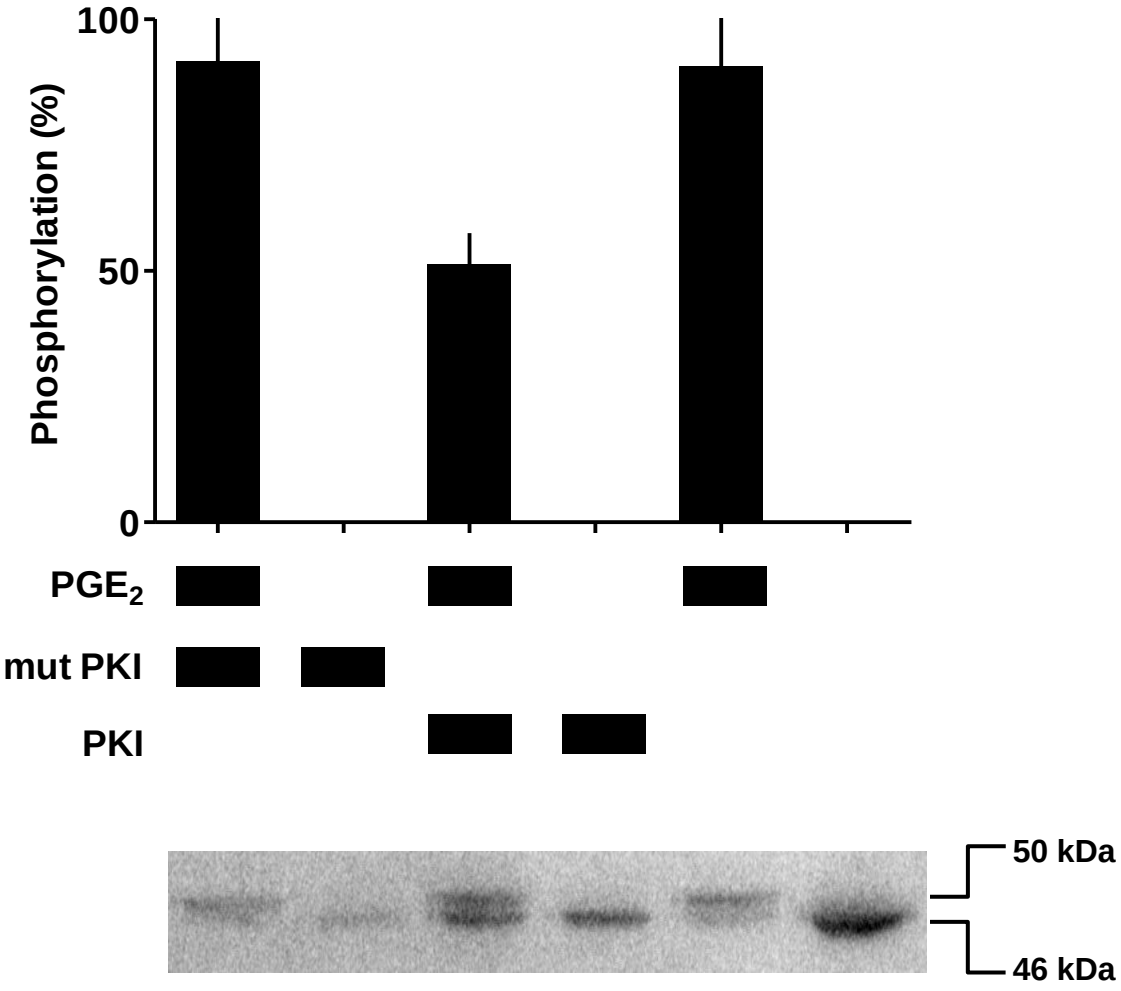

Supplemental Fig. S3. Inhibition of PGE_2-evoked VASP phosphorylation by PKI. ASMC expressing PKI or mut PKI were stimulated with PGE_2 (100 nM, 5 min). VASP phosphorylation was then determined using immunoblots with VASP clone 43 antiserum, which detects both non-phosphorylated VASP (46 kDa) and VASP phosphorylated at Ser-157 (50 kDa). Phosphorylation (%, means ± SD from 3 experiments) is reported as the shift in M_r from 46 to 50. A representative immunoblot is also shown.

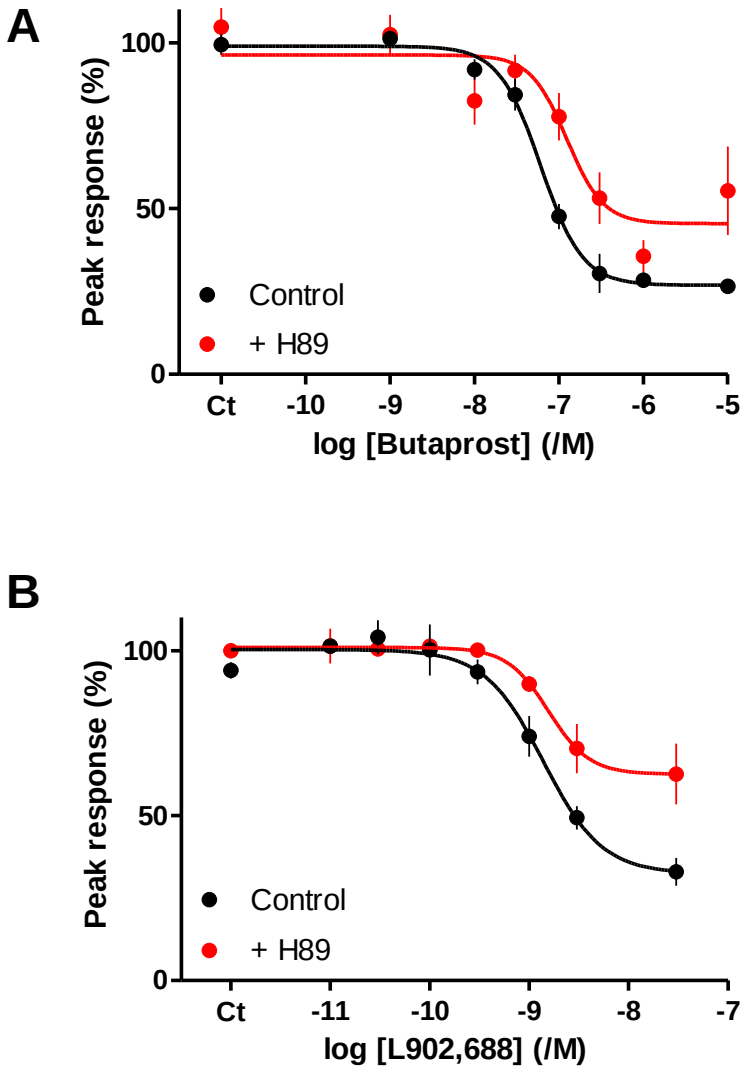

Supplemental Fig. S4. Effects of H89 on the inhibition of histamine-evoked Ca^{2+} signals by EP_2 and EP_4 receptors. (A, B) Concentration-dependent effects of butaprost (A) and L902,688 (B) on the peak Ca^{2+} signals evoked by histamine (3 μM) with or without prior treatment with H89 (10 μM, 20 min). Results are means ± SEM from 3 (A) and 6 (B) experiments with 2-5 wells in each.

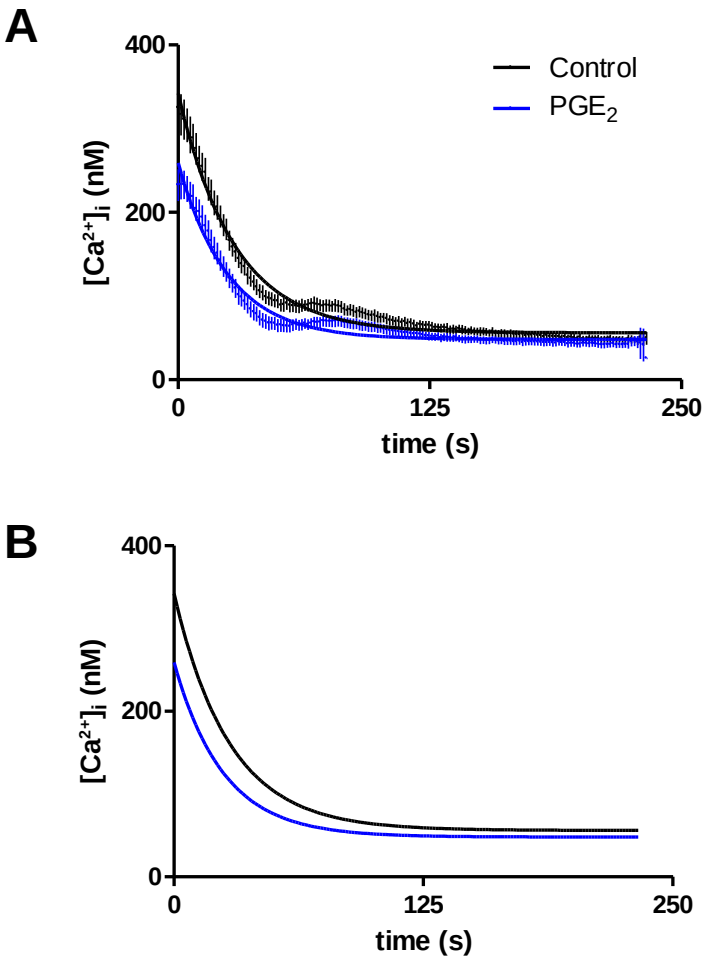

Supplemental Fig. S5. PGE_2 does not affect the rate of Ca^{2+} removal from the cytosol. (A) ASMC were stimulated with histamine (1 mM) alone or after treatment with PGE_2 (10 μM). The decaying phases of the Ca^{2+} signals after the peak response are shown as means ± SEM from 11 experiments with 1-3 wells in each. Solid lines show the mono-exponential curve-fits. (B) The curve-fits are shown without the raw data.

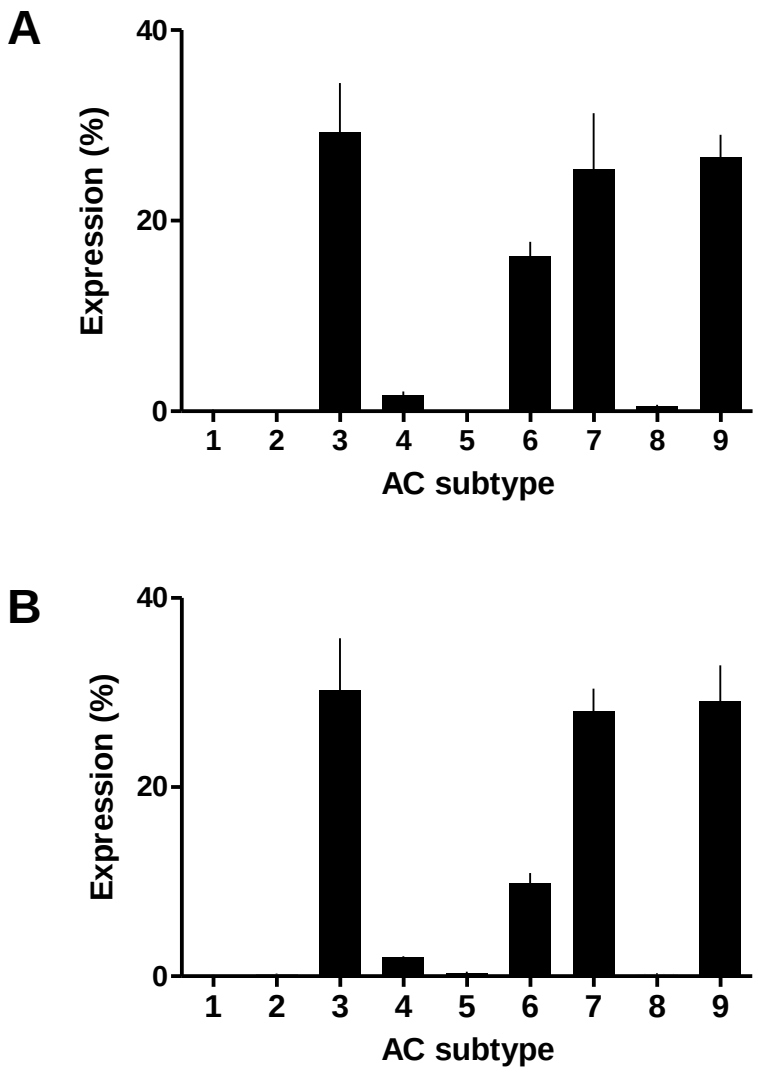

Supplemental Fig. S6. Expression of AC subtypes in human ASMC analysed by QPCR. (A, B) Relative expression levels of AC subtypes (%, means ± SEM) for cells derived from the patient (female, aged 58) used for most functional analyses (A, n = 4) or from another patient (male, aged 23) (B, n = 3). The effectiveness of the primers used for QPCR of all AC subtypes was verified using cDNA pooled from a variety of human tissues (see *Materials and Methods*).

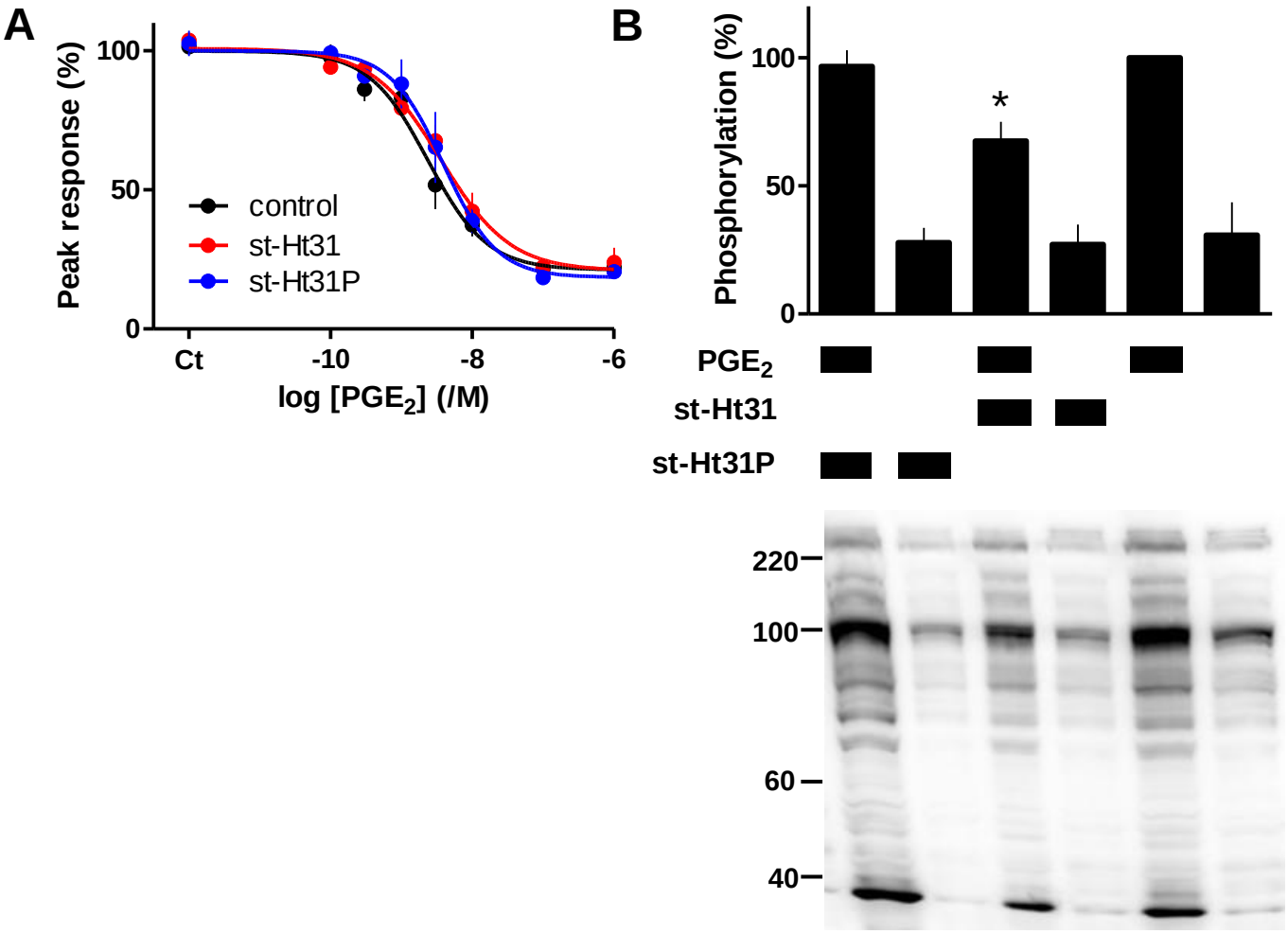

Supplemental Fig. S7. Uncoupling AKAPs from PKA does not affect inhibition of histamine-evoked Ca^{2+} signals by PGE_2. (A) Effects of PGE_2 (5 min) on the Ca^{2+} signals evoked by histamine (3 µM) in cells treated with st-Ht31 (50 µM, 20 min) or the control peptide st-Ht31P (50 µM, 20 min). (B) Typical immunoblot showing the effects of the indicated treatments (conditions as in A) on protein phosphorylation detected using AbP2 (see *Methods*). M_r markers (kDa) are shown alongside the gel. Summary results (means ± SD, n = 3) show the band intensities from across the entire gel as percentages of that from cells stimulated with only PGE_2. $^*P < 0.05$, relative to PGE_2 alone, repeated measures one-way ANOVAR with Bonferroni correction.